የኢፌዲሪ የቴክኒክና ሙያ ስልጠና ኢንስቲትዩት
FDRE TECHNICAL & VOCATIONAL TRAINING INSTITUTE

TECHNICAL AND VOCATIONAL TRAINING INSTITUTE (TVTI)

School of Graduate Studies

Thesis submitted to

FACULTY OF ELECTRICAL AND ELECTRONICS TECHNOLOGY AND INFORMATION AND COMMUNICATION TECHNOLOGY (DEPARTMENT OF ELECTRICAL AND ELECTRONICS TECHNOLOGY)

Performance Comparison of Temperature Profile Control of Clay Kiln for Ethiopian Pottery Industry

MSc Thesis for the Partial Fulfillment of the Requirements for the degree of Master of Science in Electrical Automation and Control Technology Management

By,

NAHOME NIGUSSIE (TTMR/177/16)

Advisor,

Dr. YOHANNES HAILEMESKEL

MAR, 2026

Addis Ababa, Ethiopia

የኢፌዴሪ የቴክኒክና ሙያ ስልጠና ኢንስቲትዩት
FDRE TECHNICAL & VOCATIONAL TRAINING INSTITUTE

Thesis submitted to

TECHNICAL AND VOCATIONAL TRAINING INSTITUTE (TVTI)

FACULTY OF ELECTRICAL AND ELECTRONICS TECHNOLOGY AND INFORMATION AND COMMUNICATION TECHNOLOGY

(DEPARTMENT OF ELECTRICAL AND ELECTRONICS TECHNOLOGY)

MSc Thesis for the Partial Fulfillment of the Requirements for the degree of Master of Science in Electrical Automation and Control Technology Management

By,

NAHOME NIGUSSIE (TTMR/177/16)

Advisor,

Dr. YOHANNES HAILEMESKEL

MAR, 2026

Addis Ababa, Ethiopia

DECLARATION

I hereby declare that the work presented in this thesis entitled “Performance comparison of Temperature Profile Control of Clay Kiln for Ethiopian Pottery industry ” is the original work of my own, has not been presented for a degree in this or other universities and all sources of materials used for this thesis work have been fully acknowledged.

Name: Nahome Nigussie (TTMR/177/16)

Signature: ________________________

Place: Addis Ababa

Date of Submission: ________________

This thesis submitted for examination with my approval as a TVTI advisor.

Dr. Yohannes Hailemeskel	____________________	__________________
Advisor Name	Signature	Date

TECHNICAL AND VOCATIONAL TRAINING INSTITUTE (TVTI)

FACULTY OF ELECTRICAL AND ELECTRONICS TECHNOLOGY AND INFORMATION AND COMMUNICATION TECHNOLOGY
(DEPARTMENT OF ELECTRICAL AND ELECTRONICS TECHNOLOGY)

A Thesis On

Performance Comparison of Temperature Profile Control of Clay Kiln for Ethiopian Pottery Industry

By,

NAHOME NIGUSSIE (TTMR/177/16)

APPROVED BY THESIS ADVISORY COMMITTEE

Name of Advisor	Signature	Date
Dr. Yohannes Hailemeskel	__________	__________
Name of Examiner, Internal	Signature	Date
__________	__________	__________
Name of Examiner, External	Signature	Date
Tesfaye Deme Tolossa		21/03/2026
Name of Chairperson	Signature	Date
__________	__________	__________

ACKNOWLEDGEMENT

First, I would like to say my heartfelt appreciation to my advisor Dr.Yohans Hailemeskel, for his guiding and providing constructive ideas in doing this thesis work and I would not accomplish the current achievements and finish this thesis without his guidance, patience and tolerance.

In additional, I should address my thanks for Dr.Saravanakumar Gurusamy, for his advice and support and his comments really helped me to work hard on my thesis. Finally, I would like to express my heartiest appreciation to, my family and my friends for their encouragement, cooperation and support, who are always there when it matters most.

ABSTRACT

Pottery production plays an important cultural and economic role in Ethiopia; however, traditional clay kilns are commonly operated using manual temperature control methods that lead to inconsistent firing conditions, poor product quality, and high energy consumption. Maintaining an accurate temperature profile during the firing process is critical for achieving proper clay vitrification, minimizing defects, and improving overall production efficiency. This study focuses on the modeling, design, and performance comparison of temperature profile control strategies for an electric clay kiln used in the Ethiopian pottery industry. A dynamic mathematical model of the electric clay kiln was developed based on energy balance principles, incorporating heat transfer through conduction, convection, and radiation, as well as thermal inertia and time delay effects. Using this model, three control strategies Proportional Integral Derivative (PID), Fuzzy Logic Control (FLC), and Model Predictive Control (MPC) were designed and implemented in MATLAB/Simulink. For the bisque firing process, the PID controller produced the highest tracking error with IAE of 3.82×10^4 °C·s, RMSE of 6.75 °C, and energy consumption of 128.4 kWh. The fuzzy logic controller improved performance with IAE of 2.41×10^4 °C·s, RMSE of 4.12 °C, and energy usage of 116.7 kWh, while the MPC controller achieved the best performance with the lowest IAE of 1.12×10^4 °C·s, RMSE of 1.95 °C, zero overshoot, and minimum energy consumption of 104.2 kWh. Similarly, in the glaze firing process, the PID controller recorded IAE of 4.65×10^4 °C·s, RMSE of 9.20 °C, and energy consumption of 176.5 kWh, whereas the fuzzy controller reduced these values to 3.02×10^4 °C·s**,** 5.85 °C, and 158.2 kWh, respectively. The MPC controller again demonstrated superior performance with the lowest IAE of 1.58×10^4 °C·s, RMSE of 2.80 °C, zero overshoot, and the lowest energy consumption of 142.6 kWh**.** The results indicate that advanced control strategies, particularly MPC, significantly improve temperature tracking accuracy and energy efficiency in electric clay kilns. This study provides a practical foundation for upgrading traditional kiln control systems and supports the modernization and sustainability of the Ethiopian pottery industry.

Keywords: Clay kiln, Temperature profile control, PID controller, Fuzzy logic control, Model predictive control, Ethiopian pottery industry, MATLAB/Simulink

Table of Contents

List of Figures

List of Table

Acronyms

PID	Proportional, Integral, Derivative
MPC	Model Predictive Control
SMC	Sliding Mode Control
IAE	Integral of Absolute Error
FLC	Fuzzy Logic Control
SGA	Self-tuning Genetic Algorithm
IAE	Integral Absolute Error
RMSE	Root Mean Square Error
FPFC	Fractional order Predictive Function Control
GA	Genetic Algorithm
VRFT	Virtual Reference Feedback Tuning
FIS	Fuzzy Inference System
ECS	Electronic Control System
MSE	Mean Square Error
DMPC	Distributed Model Predictive Control
ITAE	Integral Time Absolute Error
FFMRAC	Feed Forward Model Reference Adaptive Control
RCC	Robust Composite Control
SFC	State Feedback Control
DO	Disturbance Observer
SSE	Steady-State Error
DPT	Differential Pressure Transmitter
EC	Error Change
RLS	Recursive least square
DCS	Distributed Control System
SCADA	Supervisory control and data acquisition
ODE	Ordinary differential equation

List of Symbols

MPa	Mega Pascal
$U(t)$	Controller output
$e(t)$	Deviation signals
K_p	Proportional Gain
K_i	Integral Gain
K_d	Derivative Gain
τ_i	Integral time constant
τ_d	Derivative time constant
Σ	Summation
Ψ	Yaw
$\int$	Integration
ΔU	Control Increment
Γ	Weighting matrices
n_y	Prediction horizon
n_u	Control horizon

CHAPTER ONE

INTRODUCTION

1.1 Background of the study

Pottery production in Ethiopia is a traditional craft that has been practiced for centuries and, plays a significant role in the cultural and economic life of many communities. Ethiopian potters primarily use locally sourced clay and simple clay kilns to fire pottery. These kilns are mostly manually operated and rely on traditional firing techniques passed down through the generations [1]. Despite its cultural importance, Ethiopia's pottery industry faces several challenges related to kiln operations. Manual control of the kiln temperature often leads to irregular and uncontrolled heating, which affects the quality and durability of the pottery products. Inconsistent firing temperatures can cause defects such as cracking, warping, and incomplete firing, resulting in significant product loss and reduced market competitiveness. Moreover, the inefficiency of traditional kilns contributes to high energy consumption and environmental pollution owing the excessive use of firewood. This raises concerns about sustainability, especially in rural areas where natural resources are limited. To address these issues, there is a growing interest in improving kiln technology through better temperature control methods. Implementing advanced control strategies can help regulate the firing process, ensuring more uniform temperature profiles, enhancing product quality, and promoting energy efficiency [2]. Understanding the current status and limitations of clay kiln operation in Ethiopian pottery production is essential for developing effective solutions that can support the modernization and sustainability of this vital traditional industry.

1.1.1 Properties of Clay

Clay is a fine-grained natural material composed primarily of hydrous aluminum silicate minerals such as kaolinite, illite, and montmorillonite. These minerals provide clay with their characteristic plasticity, which allows them to be molded into different shapes when mixed with water. The small size and plate-like structure of clay particles enable them to slide past one another, providing the necessary flexibility for shaping. This plasticity is essential for potters, because it enables them to create complex forms that maintain their shape before firing [3].

Another important property of the clay is its shrinkage. Clay tends to shrink during drying and firing because of the loss of water and the rearrangement of particles. This shrinkage must be carefully managed to prevent cracking or warping of the pottery. Porosity is another critical characteristic; raw clay is porous, allowing it to absorb water, but firing reduces this porosity by causing verification, which binds particles together and creates a denser, less permeable material.

The chemical composition of Clay also affects its behavior during firing. The presence of minerals such as iron oxide influences the final color of the fired pottery, which can range from white and buff to red and brown depending on the clay's origin and firing atmosphere. The plastic limit and particle size of the clay further influence its workability and drying characteristics.

1.1.2 Electrical Clay Kiln

An electrical clay kiln is a specialized oven designed to heat pottery at high temperatures by using electrical resistance elements. It provides precise control over the heating process, allowing potters to follow the exact temperature profiles for consistent results. The kiln chamber is made of heat-resistant materials such as firebricks or ceramic fiber insulation, which retain heat efficiently and protect the external structure from damage. Inside the kiln, electrical heating elements made from alloys such as nichrome or kanthal convert electrical energy into heat through resistance. These elements were strategically arranged to distribute the heat evenly throughout the chamber. Temperature sensors, commonly thermocouples, monitor the internal temperature [4-5].

The firing cycle in an electrical kiln typically begins with a slow drying phase where the temperature is gradually increased to approximately 200°C to evaporate free water from the clay body. This is followed by a dehydration phase, where temperatures rise to between 850° and 950°C to remove chemically bound water and burn off organic materials. The kiln then enters the sintering and vitrification stage, where temperatures reach between 1150°C and 1260°C depending on the type of clay and the desired properties of the finished product. During this stage, the clay particles fuse together, and the ceramic body becomes hard and durable. Finally, the kiln gradually cools to prevent thermal shock, which can cause cracking [6-5].

Compared to traditional wood-fired kilns, electrical kilns offer several advantages, including cleaner operation without combustion gases, greater energy efficiency owing improved insulation and control, and enhanced safety. Their ability to precisely control firing temperature and timing improves the quality and consistency of the final pottery products.

1.1.3 Fired Clay

Fired clay, often referred to as ceramic, results from subjecting shaped clay to high temperatures in a kiln, triggering physical and chemical transformations that harden the material. During firing, the clay undergoes several important changes. First, all the free and chemically bound water was removed. Next, the organic materials within the clay burned out. The clay minerals then decompose and reorganize into more stable phases. One example is the transformation of kaolinite into metakaolin and then mullite at high temperatures. As the temperature increases, particles in the clay begin to sinter and, fuse at the grain boundaries, which strengthens the body and reduces porosity. Vitrification occurs when silica and other fluxing agents partially melt, creating a glassy matrix that binds particles together and, enhance strength and water resistance [7].

Fired clay products can be classified into earthenware, stoneware, and porcelain based on their firing temperature and characteristics. Earthenware is fired at relatively low temperatures and remains porous and weak. Stoneware, fired at higher temperatures, was denser, harder, and more durable. Porcelain is highly vitrified, white, and often translucent and, represents the highest firing quality [7-8].

1.1.4 Characteristics of Fired Clay

Fired clay possess several distinct characteristics that determine their suitability for various applications. Mechanically, fired clay has high compressive strength, which allows it to withstand loads without deformation. Its surface hardness was significantly increased, making it resistant to scratches and abrasion. However, ceramics are brittle materials that can fracture under tensile or impact stresses. Thermally, fired clay is stable at high temperatures and does not easily melt or deform. However, the resistance to thermal shock varies depending on the clay composition and firing process; sudden temperature changes can cause cracking in some ceramics. The physical properties of the fired clay also significantly changed. The density increased owing the reduction in porosity during firing, making the material stronger and less permeable to water. The color of fired clay is influenced by the mineral content and firing atmosphere, with iron oxides producing hues from reddish-brown to buff and white clays resulting in lighter colors[9]. Chemically, fired clay becomes inert and resistant to many environmental factors, such as chemical attack and weathering. This chemical stability contributes to the longevity of pottery products used for cooking, storage, and decoration. In addition to these functional properties, fired clay can have various surface textures, ranging from smooth to rough, depending on the clay composition and firing conditions[10]. The application of glazes can further enhance the aesthetic appeal and water resistance of the fired products.

1.2 Statement of the Problem

In Ethiopia, traditional clay kilns remain vital to rural pottery production, yet they are typically operated manually, relying heavily on artisans' experience to control the temperature during the firing process. This subjective approach often leads to inconsistent temperature profiles, resulting in defects such as cracking, under-firing, and product deformation, while also contributing to significant energy inefficiency. The absence of reliable and adaptive control systems limits the product quality, consistency, and the economic viability of pottery businesses in the local markets. Modern research on thermal systems has demonstrated that intelligent controllers are more effective than traditional Proportional-Integral-Derivatives (PID) controllers in managing the nonlinear behavior and time delays inherent in kiln operations. These advanced techniques offer an improved accuracy and energy efficiency. However, their application in the Ethiopian context is rare, primarily because of their complexity, cost, and lack of customization for traditional, small-scale kilns. This study aims to address this gap by modeling an electric clay kiln and designing various temperature control systems. The objective is to simulate the key firing phases of bisque, and glaze and evaluate the controller performance. By comparing the energy efficiency and temperature stability of different control strategies, this study will recommends a suitable and, cost-effective control solution for traditional kilns.

1.3 Objectives of Thesis

1.3.1 General Objective

- Design and simulate PID, fuzzy and MPC based temperature profile control systems for clay kilns in Ethiopian pottery production and also comparison of their performance.

1.3.2 Specific Objectives

- To design mathematical model for electrical kiln.
- To design PID, fuzzy and MPC controllers for simulating key phases of the firing process.
- To simulate typical firing profiles (bisque and glaze firing stages)
- To compare the performance of PID, FUZZY and MPC controllers and assess the controllers performance for energy efficiency and recommend a suitable controller for the clay kiln.

1.4 Scope

This thesis is limited to the theoretical modeling and simulation of a temperature control system for an electric clay kiln, focusing specifically on its application in the Ethiopian pottery industry. This study aimed to design and analyze a suitable temperature regulation method that can effectively follow the desired firing profile required for clay vitrification and sintering. All work will be carried out using MATLAB and Simulink, without any physical implementation or hardware construction.

1.5 Limitation

The limitations of the temperature profile controller for clay kilns in the Ethiopian pottery industry discussed in this thesis, the system is limited to MATLAB/Simulink simulation only and it could not implement in prototype and practically.

1.6 Thesis Organization

This thesis is organized into six chapters.

Chapter One: presents the introduction, including the background of the study, properties of clay, electrical clay kiln, fired clay, characteristics of fired clay, Statement of the problem, objectives, as well as the scope and limitations of the study.

Chapter Two: provides the literature review, covering the general overview and related works relevant to the study.

Chapter Three: describes the methodology and system design, including the mathematical modeling of the electrical kiln and the analysis of heat flow rate.

Chapter Four: focuses on the controller design, including Proportional–Integral–Derivative (PID), Fuzzy Logic, and Model Predictive Control (MPC) controllers.

Chapter Five: presents the simulation results and discussion of the system performance.

Chapter Six: concludes the study and provides recommendations for future work.

CHAPTER TWO

LITERATURE REVIEW

2.1 Related Works

Stojanovski et al. (2011) this academic paper exploreds advanced control methods for complex industrial heating processes, specifically focusing on a tunnel kiln for brick production at the "KIK" factory in Kumanovo. The authors proposed a two-level hierarchical control system that combines Model Predictive Control (MPC) for temperature regulation and Fuzzy Logic control to improve brick quality based on factors such as color, porosity, and mechanical hardness. The simulation results, using a MATLAB Simulink model of the kiln, indicate that this fuzzy-MPC approach is effective in maintaining the desired temperature profiles, reducing fuel consumption, and ultimately enhancing the quality of the final brick product compared to conventional control systems[11].

Eskelinen et al. (2015) described the creation and testing of a dynamic model for a multiple hearth furnace (MHF) used in kaolin calcination. The researchers developed a model considering the physico-chemical processes across six furnace parts, incorporating a novel mixing model for solid material movement based on pilot experiments. The model was validated using industrial data and analyzed for its dynamic behavior in response to changes in inputs, such as feed rate and air flows, providing insights into temperature and solid composition profiles to potentially optimize furnace control for better product quality [12].

Adar Bakhsh Baloch et al. (2017) focused on developing a new temperature profile control strategy for a multiple hearth furnace (MHF) used in kaolin calcination with the, aim of improving product quality. This study proposes a multi-level control hierarchy, reviews existing literature on furnace temperature control (including techniques such as decouplers, cascade control, and Model Predictive Control), and conducts a data-based analysis of the MHF's operating conditions. A key finding from the data analysis is the impact of the exothermic reaction in hearth 4 on the furnace's temperature profile. To address this, this thesis develops a soft sensor based on energy balance to estimate the intensity of this crucial reaction and, a comparison showing that a dynamic energy balance provides more accurate estimations than a static one by considering the process dynamics and residence time[13].

Zhang et al. (2017) described improving the notoriously difficult temperature regulation within industrial ceramic kilns. Recognizing that conventional PID control methods cannot stabilize systems facing large time delays and internal disturbances, the paper proposes and designs an advanced control strategy. This solution involves implementing a fuzzy PID adaptive control algorithm supported by hardware utilizing an ARM microprocessor and highly precise temperature sensors. The methodology first requires establishing the extensive mathematical modeling and transfer functions necessary to accurately represent the complex heating and air-flow characteristics of the kiln environment. Ultimately, simulation and real-world application confirmed that the proposed fuzzy adaptive controller successfully met the system's demands, resulting in stable and accurate temperature control validated by years of practical operation [14]. Eshetu Tsega et al. (2017) investigated how variations in firing temperature and duration impact key physical properties specifically compressive strength (CS), water absorption (WA), and saturation coefficients (SC) of clay bricks produced in Ethiopia. The study found that increasing the firing temperature generally improved compressive strength while simultaneously decreasing water absorption and saturation coefficients, confirming that firing parameters significantly affect the engineering quality of the bricks. The authors also highlight that traditional producers in the Jimma area often lack proper temperature control devices, leading to inconsistent brick quality, and they recommend that producers either install controls or receive adequate training [7].

Y Zhang et al. (2018) This document details a research paper proposing a fuzzy PID control method for precisely regulating the temperature within a resistance furnace, which is known for challenging control dynamics like large time delay and inertia. The authors argued that traditional PID methods fall short in such systems, and their fuzzy PID approach dynamically adjusts PID parameters based on real-time temperature errors and error rates. Through simulation, they demonstrate that this enhanced control results in a faster, more stable, and robust system with improved accuracy and disturbance rejection compared with conventional PID control. The study concludes that this fuzzy PID method offers a promising solution for achieving high-precision temperature control in resistance furnaces [15].

Cantore et al. (2018) described a numerical analysis of an industrial ceramic kiln, constructed to investigate strategies for improving energy efficiency and reducing fuel consumption and emissions. Researchers utilized a lumped and distributed parameter model (0D/1D) to accurately simulate the complex system, devoting particular attention to modeling detailed heat transfer phenomena like conduction, convection, and radiation. The simulation's capabilities, including its accurate prediction of gas and tile temperature profiles, were validated against experimental measurements taken from a functioning production facility. Once validated, the model was employed to explore optimization solutions, such as the injection of gas turbine exhausts to enhance heat exchange during the pre-heating phase, achieving a measurable reduction in natural gas consumption. Finally, the numerical approach successfully analyzed the kiln's dynamic behavior, allowing calculation of warm-up and cool-down times and fuel usage during unforeseen stand-by operations [16].

Machalek et al. (2019) this document explores the use of model predictive control (MPC) to allow rotary kilns, typically operated steadily owing high thermal inertia, to respond flexibly to rapid changes in electric demand. By dynamically adjusting inputs such as the rotation rate and stone/coal feed rates, the MPC algorithm successfully minimizes process disruptions and maintains high product quality even during the significant power fluctuations required for smart grid participation. This study demonstrates that this approach significantly reduces the economic penalty of these responses compared to simply changing to a new steady state, highlighting the potential for mineral processing facilities to become valuable grid assets [17].

Baccour et al. (2019) investigated the effect of varying firing temperatures affect the ceramic properties of Triassic clays found in southeastern Tunisia, focusing on their potential for faience ceramic production. This study meticulously analyzed the mineralogical and physico-chemical characteristics of the clay, identifying key components such as illite, kaolinite, quartz, dolomite, and hematite, and then observed how these properties, such as densification, water absorption, and mechanical strength, change when the clay samples are heated to different temperatures. These findings suggest that the specific composition of these Tunisian clays, particularly their iron oxide content and flux materials, can promote rapid vitrification at elevated temperatures, leading to improved strength and reduced water absorption, thus making them suitable for the production of ceramic faience [18].

Steve Nagorsky et al. (2020) described the macro- and micro archaeological investigation of a pottery kiln at Tel Qatra/Gedera, Israel, dating to the Late Byzantine and Early Islamic periods (7th century CE). The structure was unusual because it lacked the common architectural features of ancient kilns, requiring identification based on its contents and surrounding heat-altered sediments. Researchers utilized detailed analytical methods to study the ash and debris, which revealed that the kiln primarily used the stalks and chaff of domesticated grasses, likely wheat, as its fuel source. Analysis of the partially recrystallized phytoliths silica bodies from the plants showed the formation of the high-temperature mineral cristobalite and slags, indicating sustained firing temperatures between 700 and 900 °C. This comprehensive micro archaeology study was essential for characterizing the poorly preserved kiln and reconstructing its basic design, which featured an unpartitioned pottery chamber situated above the firing area [19].

Ravi et al. (2021) described a comprehensive energy audit and subsequent technical improvement of traditional, firewood-burning updraught pottery kilns used extensively by rural craftspeople. Initial studies on two kilns demonstrated extremely low efficiency, with the majority of the combustion energy being absorbed by the kiln's massive thermal structure or lost through escaping flue gases. To address this issue, an improved updraught kiln was developed that utilized a lighter, insulated design incorporating rat-trap bonded walls and air gaps to minimize structural heat absorption. This innovative redesign proved highly successful, achieving a reduction in fuel consumption by about 50% per kilogram of pottery fired compared to the original design. Furthermore, the new construction method resulted in a lower capital cost of construction, making the energy-efficient technology economically viable for small-scale potters and offering potential for significant nationwide energy conservation [20].

Tseligorov et al. (2021) this document presents research on improving the temperature control system for tunnel kilns, which are used in processes like firing sanitary ware and bricks. Traditional PID controllers struggle with the complex characteristics of the kiln, such as its non-linear temperature behavior and inherent delays. Therefore, the authors propose the integration of a fuzzy logic controller with a conventional PID controller to create a more robust and stable system that effectively manages temperature fluctuations. Through simulation, this fuzzy PID control approach demonstrated improved performance by reducing overshoots and enhancing stability compared to a standard PID setup [21].

Govind et al. (2022) described high fuel consumption and poor product quality resulting from the use of traditional pottery kilns in small-scale rural industries in India. The study aimed to optimize the design of an improved downdraught kiln to achieve better temperature uniformity and decrease fuel usage during the burning process. Since practical construction and testing would be expensive, the authors employed Computational Fluid Dynamics (CFD) modeling, utilizing ANSYS Fluent software to analyze heat transfer and flue gas flow. The simulation specifically examined the impact of varying the firewall height, chimney height, and roof geometry on kiln performance during the rapid firing stage. The conclusions indicate that optimal thermal performance and even temperature distribution are achieved in a model featuring a 0.75 m firewall height**, a** 5 m chimney height, and a dome roof with a larger radius of curvature [22].

Sachin Makarande et al. (2022) provided a comprehensive overview of the design evolution and current challenges facing traditional kilns used in the small-scale pottery industry. The research systematically details various historical designs, including bonfire kilns and different generations of up draught, downdraught, and cross-draught kilns, explaining the structural and thermal limitations of each. A primary finding is that traditional kilns relying on firewood are highly inefficient, resulting in extensive product breakage, non-uniform temperatures, and significant health risks from smoke exposure. To further highlight these deficiencies, the text contrasts these rudimentary methods with modern alternatives like gas and oil fired kilns, which achieve the precise, high temperatures required for quality glazed wares. The authors conclude that overcoming these widespread thermal shortcomings necessitates the urgent development of a new, energy-efficient pottery kiln design featuring improved structural stability and better insulation [23].

Olabode et al. (2022) investigated the use a Fuzzy Logic Controller (FLC) to manage the temperature in a cement kiln, aiming for improved clinker quality and reduced production costs compared with traditional proportional-integral-derivative (PID) controllers. The FLC employs a three-stage process: converting data to fuzzy sets (fuzzification), processing information through an inference system, and translating fuzzy outputs back to understandable data (defuzzification). While PID controllers are widely used, their struggle with the nonlinear nature of kilns can lead to suboptimal products and inefficiencies and issues the FLC addresses by eliminating overshoot and undershoot in temperature control. The study concludes that the FLC offers a superior and more autonomous solution for kiln temperature control, recommending its application for optimal performance [24].

Shakya et al. (2022) analyzed the performance metrics, including specific energy consumption and heat loss, of two established sites: the Gathaghar and Everest pottery furnaces. The analysis concluded that the Everest furnace was more efficient in its original state, prompting its selection for further engineering modification. The improvement process involved constructing an additional insulating wall of fire brick to minimize thermal energy escaping through the outer surfaces. Validation using experimental data and ANSYS software confirmed that this structural enhancement successfully decreased heat loss and consequently increased the overall efficiency of the modified furnace by significant margins [25].

Namaswa et al. (2023) investigated the suitability of various kiln designs for small-scale biochar production in low to middle income countries (LMICs), where efficient use of agricultural waste is critical but expensive technologies are impractical. The text meticulously categorizes and compares existing designs, such as simple flame curtain kilns, drum kilns, and more complex retort systems, based on metrics like efficiency, biochar quality, investment cost, and resulting emissions. The authors note that the selection of any kiln involves a fundamental trade-off between low initial cost and overall system performance and control. While simpler methods are cheap, they often lead to highly heterogeneous biochar and significant pollution, whereas modern automated systems are prohibitively expensive for local farmers [26].

Dechpratoom et al. (2023) presented presents a study analyzing the thermal distribution patterns within a commercial 3.6 m^3 downdraft ceramic kiln. The research addresses the common industrial problem of uneven firing, which results in high waste product rates because the temperature gradient is steep, with the roof significantly hotter than the base. To understand the internal environment, researchers employed a two-pronged methodology, combining physical measurements using thermocouples and Pyrometric rings with Computational Fluid Dynamics (CFD) modeling to accurately map internal temperatures and air flow. The CFD simulation proved reliable, showing alignment with measured data and identifying major temperature volatility, particularly within the middle and lowest levels of the firing chamber. Specifically, the investigation observed that the flow of hot gases was imbalanced toward the rear exit, indicating that improvements to air flow management are necessary to achieve uniformity and maximize utilization of the kiln volume [27].

Sopa Pattiya et al. (2023) investigated methods for improving the inconsistent brick quality commonly observed in industrial downdraft kilns, a problem frequently caused by uneven temperature distribution during the firing process. The study proposes a simple, accessible solution: inserting various solid media, including alumina balls, clay balls, and sandstone sheets, into the spaces between the raw clay bricks to assist with heat reflection and distribution. Experimental testing demonstrated that this technique was highly effective, particularly when using alumina balls combined with sandstone sheets, which reduced the temperature difference between the top and bottom kiln sections from a drastic 344°C to an optimal 23°C. This enhanced thermal uniformity led to stronger products, as the method successfully significantly enhanced the compressive strength of the fired bricks, nearly doubling that of typical industry standards. Consequently, this simple implementation using locally available materials offers a practical way for manufacturers to increase product reliability and reduce the overall percentage of damaged or inferior bricks [28].

Laurini et al. (2024) proposed a theoretical framework for electrifying the clay calcination process in cement plants, with the aim of reducing CO2 emissions by integrating these electrified plants with sustainable power grids. The core aim of this research is to develop a dynamic model to simulate the calcination process and an energy management system (EMS) to optimize energy usage within the plant, considering factors such as cost, emissions, and technical constraints. This study highlights how this integrated approach can effectively manage the increased electricity demand from electrification and efficiently utilize renewable energy sources, ultimately paving the way for more environmentally friendly cement production [29].

V Moreno et al. (2024) described the development and verification of a thermal model designed to accurately estimate both surface and internal temperature profiles of ceramic tiles throughout the industrial firing cycle. Researchers from the Instituto de Tecnología Cerámica created a theoretical framework that incorporates heat transfer mechanisms like convection and radiation from the kiln environment, along with heat conduction within the tile itself. To validate the calculations, experimental measurements were conducted using specialized temperature probes and thermocouples placed directly on tiles inside a commercial roller kiln. The results revealed pronounced discrepancies, sometimes exceeding 200 ºC, between the monitored kiln gas temperature and the actual tile surface temperature, especially during rapid heating or cooling phases. Furthermore, the study confirmed that rollers significantly impede heat transmission, and calculated data showed large temperature differentials between the tile's core and its surface during cooling, critically impacting material properties and stress development [30].

D Cerarnica et al. (2024) analyzed and control firing conditions in industrial ceramic roller kilns. Recognizing that traditional measurement methods fail to capture crucial spatial variations, the research focused on determining the precise transverse temperature gradients occurring beneath the roller plane, which are significantly closer to the actual tile temperature. Using this specialized thermocouple-equipped roller, the researchers mapped temperature profiles through the preheating and firing zones, demonstrating that considerable temperature non-uniformities exist, especially near the kiln walls. A core objective was to assess the impact of modifying three key operating conditions the number of lighted burners, the combustion air pressure, and the gas static pressure on these thermal gradients. The experiments concluded that strategically altering these parameters, such as raising the gas static pressure, can slightly mitigate temperature differences, thus offering manufacturers better control over tile quality and reducing product defects [31].

Phan et al. (2024) This academic article, "Development of an Adaptive Fuzzy-Neural Controller for Temperature Control in a Brick Tunnel Kiln," explores the creation and testing of a sophisticated system to precisely regulate the temperature within kilns used for firing bricks. Recognizing the limitations of traditional methods, the researchers have proposed an innovative adaptive fuzzy-neural control approach that combines the strengths of fuzzy logic (handling uncertainty) and neural networks (learning capabilities) to improve the efficiency and reduce energy use. Through simulations and experiments, they demonstrate that this advanced controller significantly enhanced the temperature control accuracy and overall brick production performance compared with existing PID and standard fuzzy controllers [32].

Silvia Cuccui et al. (2024) presented a hybrid active indirect kiln dryer that utilizes solar and biomass energy for heating, along with photovoltaic panels to supply electricity for fans and controls. The kiln chamber was intentionally constructed using 100% biodegradable, local materials like vetiver grass, wood, and clay to promote replicability and social benefits within the artisanal logging community. Preliminary testing demonstrated that the supplementary power provided by the biomass furnace significantly improved the drying rate from 0.4% to 1.4% per day compared to relying solely on solar energy, although the high upfront costs of the photovoltaic system were noted as the main factor influencing the total investment. The overall project aims to enhance the artisanal timber value chain by introducing a more efficient and sustainable wood seasoning method [33].

Ceccarelli et al. (2025) this scientific article explores the mineralogical transformations that occur in clays from a Roman ceramic workshop in Umbria, Italy, are fired, aiming to understand ancient pottery technology. By conducting experimental firing of these specific clays and comparing the results to actual Roman amphorae found at the site, the researchers were able to estimate the firing temperatures used by ancient potters, likely around 900°C. This study highlights how the clay composition, particularly the amount of calcium, influences these transformations and the final properties of the ceramics. Furthermore, the research acknowledges that post-burial alterations can impact the mineral content of ancient ceramics, which requires careful consideration when determining the original firing conditions [34].

Rasha Mohammed et al. (2025) described the development and application of an intelligent electric ceramic kiln equipped with an advanced control system intended to modernize the firing process. The system utilizes an ESP32 microcontroller and K-type thermocouples to achieve precise temperature regulation up to 1000°C across ten distinct stages. A key feature is the advanced control panel, which supports both manual inputs and remote operation via Wi-Fi, allowing users to optimize firing curves and log data in real-time. Experimental results confirmed the success of the applied study, demonstrating significantly enhanced product integrity and stability while achieving an impressive 80% energy efficiency rate. The authors conclude that this smart kiln technology offers a sustainable and efficient solution for consistent, high-quality ceramic production, positioning it as a substantial upgrade over conventional heating systems [35].

2.2 Summary of Literature Reviews

The literature reveals significant progress in the development of advanced temperature control methods for kilns and furnaces used in ceramics, cement, clay and mineral processing. Traditional PID controllers often fall to manage the nonlinear behavior, time delays, and thermal inertia of these systems. To overcome these challenges, researchers have introduced intelligent and hybrid control strategies. Fuzzy-PID controllers have shown improvements in stability, accuracy, and responsiveness by adjusting the parameters in real-time based on process variations. More sophisticated approaches, such as adaptive fuzzy-neural controllers, combine fuzzy logic and neural networks to further enhance precision and energy efficiency. Model Predictive Control (MPC) has also been widely applied because of its ability to handle multivariable systems with constraints and disturbances, making it effective in dynamic environments and integration with energy demand management. Dynamic modeling and soft sensors based on energy balance equations are increasingly being used to monitor and simulate thermal processes, providing critical insights for optimizing control. These models support the real-time estimation of internal conditions and improve process predictability. In the context of sustainability, integrated systems that manage energy consumption and emissions have been proposed, particularly for electrified calcination processes that are powered by renewable energy. Additionally, studies on the mineralogical behavior of clays under different firing conditions underscore the importance of tailored temperature profiles to achieve the desired material properties. Overall, the literature highlights a clear trend toward adaptive, data-driven, and energy-conscious control systems that improve the process efficiency, product quality, and environmental performance in thermal processing applications.

CHAPTER THREE

METHODOLOGY

This thesis aims to develop and compare three temperature control strategies conventional PID, Fuzzy Logic, and Model Predictive Control (MPC) for an electric clay kiln employed in traditional Ethiopian pottery making. The work focuses on accurately following the complete firing schedule that includes bisque, and glaze firing phases. Using MATLAB/Simulink as the primary simulation platform and draw.io for electrical kiln design, the research investigates the capability of each controller to maintain tight tracking of the desired temperature trajectories.

3.1 Mathematical Model of Electrical Kiln

The main goal Performance comparison of Temperature Profile Control of Clay Kiln is to provide close loop control using parameters that may be changed to change the system's response. The model is selected in a way that produces the intended, ideal process reaction. By doing this, the adjustment mechanism immediately modifies the controller parameter, enabling the given plant system to be controlled and creating tracking to a reference model that performs as intended. Figure 3.1 depicts the crucial electrical kiln system used in the clay firing process.

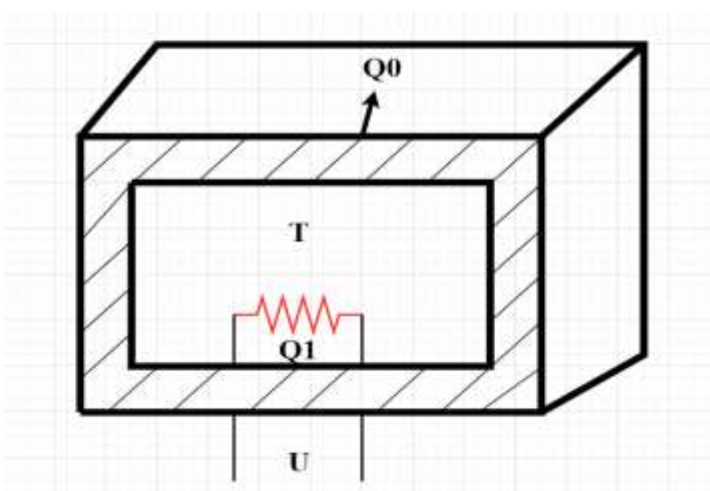

Figure 3.1: Electrical kiln

The dynamic behavior of the kiln temperature can be derived using law of energy conservation. The electrical power supplied to the kiln is used to rise the temperature of the clay kiln structure while compensating for heat losses to the surrounding.

The mathematical heat flow equation of electrical kiln is given by

$$U(t) = \mathrm{M}C_p \frac{dT(t)}{dt} + \mathrm{HA}(\mathrm{T(t)} - T_\infty)) \qquad (3.1)$$

Where,

U(t) is electrical power supplied to the kiln, M is total mass of clay and kiln structure, C_p is specific heat capacity, T(t) kiln temperature at a time t, $T_\infty$is ambient temperature, H is over all heat transfer coefficient and A is effective heat transfer area.

To design linear controllers, the nonlinear model is linearized around a nominal operating point (U_0, T_0)

$$\Delta U(t) = U(t) - U_0, \quad \Delta\mathrm{T(t)} = \mathrm{T(t)} - T_0 \qquad (3.2)$$

Substituting in to equation 3.1 and neglecting higher order nonlinear term yields the linearized model

$$\Delta\mathrm{U(t)} = \mathrm{M}C_p \frac{d(\Delta T(t))}{dt} + \mathrm{HA}(\Delta\mathrm{T(t)}) \qquad (3.3)$$

Dividing both sides by HA we can get,

$$\frac{1}{\mathrm{HA}} \Delta\mathrm{U(t)} = \frac{\mathrm{M}C_p}{\mathrm{HA}} \frac{d(\Delta T(t))}{dt} + \left(\Delta\mathrm{T(t)}\right) \qquad (3.4)$$

Where, $\frac{1}{HA} = K$ and also,$\frac{MC_p}{HA} = T$ now apply Laplace transfer function

$$\Delta\mathrm{U(s)K} = \mathrm{Ts}(\Delta\mathrm{T(s)}) + (\Delta\mathrm{T(s)})$$

$$\frac{\Delta\mathrm{T(s)}}{\Delta\mathrm{U(s)}} = \mathrm{H(s)} = \frac{\mathrm{K}}{\mathrm{Ts} + 1} \qquad (3.5)$$

Where,   is thermal time constant, K is steady state temperature gain.

The time delay represents delay between electrical power input and measurable temperature rise due to thermal inertia of the kiln structure, heat diffusion through refractory materials, actuator dynamics of heating element and sensor response delay.

$$D = D_{thermal} + D_{actuator} + D_{sensor} \tag{3.6}$$

Where,

$D_{thermal}$: Heat diffusion through kiln wall and load

$D_{actuator}$: Heat power build up delay

D_{sensor} : Thermocouple and signal processing delay

By incorporating the delay in to equation 3.5 the complete kiln model becomes:

$$G(s) = H(s) \;\; e^{-DS} = \frac{K}{TS+1}\, e^{-DS} \tag{3.7}$$

3.2 Heat Flow Rate of an Electrical kiln

Heat is the energy transferred as a result of a temperature differences and always flows from a region of higher temperature to a region of lower temperature. In an electrical clay kiln, heat generated by the electrical heating element is transferred to the kiln chamber and clay load through **conduction**, **radiation** and **convection**.

These heat transfer mechanism directly influence the kiln's thermal gain, time constant and delay.

$$Q_{in} = U_{electric} \tag{3.8}$$

Where,

Q_{in} : Heat input rate

$U_{electric}$: Electric power supplied to heating element

1.2.1 Heat transfer By Conduction

The transfer of heat from one body part at a higher temperature to another similar body part at a lower temperature, or from one body at a higher temperature to another body in physical touch with it at a lower temperature, is known as conduction. Energy is transferred from more active (energetic) molecules to those with a lower energy level during the conduction process, which occurs at the molecular level. This is easily imagined in the context of air, where we observe that molecules with average kinetic energy in the higher temperature zone have a larger average kinetic energy than molecules in the lower temperature region.

$$Rate\ of\ heat\ condition\ = \frac{(Area)(Temperature\ difference)}{Thicknees}$$

$$H_{cond} = \frac{KA(T_s - T_\infty)}{\Delta X} \tag{3.9}$$

Where,

K = 0.78W/m°C is fire clay

ΔX = 0.15m kiln wall thickness

A=4m^2

T_s=1300^{0}C

T_∞=30^{0}C

Thus, $H_{cond} = \frac{KA(T_S - T_\infty)}{\Delta X} = \frac{0.78\text{W/m°C x } 4m^2(1300-30)}{0.sm} = 17{,}035\ watt \approx 17KW$

1.2.2 Heat transfer By Radiation

Thermal radiation, often known as radiation, is electromagnetic radiation that a body emits as a result of its internal energy consumption and temperature. As a result, thermal radiation combines characteristics with radio waves, X-rays, and visible light; the only differences are in their generating sources and wave lengths. The visible spectrum, which is defined as the wavelength range between 0.39 and 0.78 $\boldsymbol{\mu}$m, is the one that the eye is most sensitive to electromagnetic radiation.

1.2.3 Heat transfer by convection

Convection, which is at times recognized as a distinct mode of heat transfer, is linked to the transfer of heat from a boundary surface to a fluid in motion or with the transfer of heat across a flow plane inside the flowing fluid. The process is known as forced convection if the fluid motion is caused by a blower, fan, pump, or other similar device; the process is known as free or natural convection in a batch electrical clay kiln, air motion inside the kiln can be caused by density differences resulting from temperature gradients, leading to natural convection. At the bottom surface of the clay, where direct heat transfer occurs from the kiln floor or heating elements, natural convection is more effective. To reduce the difference in heat transfer between the top and bottom surfaces of the clay, air-jet systems are often installed to blow air onto the top surface during firing. As a result, the overall heat transfer in the batch kiln is determined by the combined effects of conduction from the heated surfaces and convection over the clay. This is commonly accomplished for ease of use and simplicity by defining a combined heat transfer coefficient,$h_{combind}$, which considers both convection and radiation effects.

$$H_{conv\,\&\,radai} = h_{combind}A(T_s - T_\infty) \tag{3.10}$$

Where,

$h_{combind}$ is the heat transfer coefficient for radiation and convection in $W/m2$℃ take it 4.5$W/m2$℃

T_s=1300^{0}C

T_∞=30^{0}C

A=4m^2

Therefore, $H_{conv\ and\ radai} = 15{,}047 watt \approx 15kw$

In general, the total amount of heat transfer is

$$H_{cond} + H_{conv\,\&\,radi} = 32000\ watt\ =\ 32KW$$

3.3 Process Parameters

In Assumptions

The kiln chamber's volume is selected to be $V = 4m^3$

$$\text{The Length of the kiln} = 2\text{m}$$

$$C_p = 837 J/kg°C$$

$$\text{Electric power} = 32\text{KW}$$

Effective kiln + clay mass (M) = 380kg

Thermal capacitance $C_{th} = MC_p = 1.67x10^5 J/°C$

Over all heat loss coefficient *effective surface area (HA) = 0.0252Kw/℃

The constant values are

$K = 40$, $T = 3\text{h} = 10800sec$, $D = 30sec$

The electrical kiln's dynamic model for firing clay is:

$$G(s) = \frac{\Delta T(s)}{\Delta U(s)} = \frac{Ke^{-DS}}{Ts+1} = \frac{40e^{-30S}}{10800s+1} \tag{3.11}$$

The transfer function of the dynamic model is unable to capture the time delay. As a result, I may utilize MATLAB's PADE first order approximation to make the mathematical model easier

Finally, Equation we get after using in MATLAB

$$G(s) = \frac{-40s + 26.8}{10800s^2 + 721s + 0.67} \tag{3.12}$$

Electrical kiln control of temperatures for the clay firing process uses a variety of controller designs. The goal of this thesis is Performance comparison of Temperature Profile Control of Clay Kiln for Ethiopian Pottery industry.

3.4 A Reference Model of an Electrical kiln

Selection of Reference Model: In this research, I selected transfer function on electrical kiln is chosen as second order system

$$G(s) = \frac{100}{s^2 + 20s + 100} \tag{3.13}$$

The damping ratio and ω_n are the two parameters that can be used to determine the dynamic performance of the second order system. When the damping ratio is between zero and one, the closed loop poles are conjugate and lie in the left-half s plan. The temporary response is oscillatory and the system is called under damped. The system is said to as critical damped when the damping ratio is equal to zero. A system that is over-damped has a damping ratio larger than 1. A critical damped and over damped system's transient response is non-oscillating. The temporary reaction occurs even when the damped ratio is equal to zero.

3.5 Model Analyze of Electrical kiln

To analyze the model of electrical kiln adaptation mechanism is utilized adjust the parameters in control law. The adaptation law finds for the parameters this means, the plant must be similar with the reference model. It is designed to guarantee the stability of control system as well as convergence of tracking error to zero. The rule utilizes the error between the process and the model output, the process output and input signal to fluctuate the parameters of control system. These the constraint varied so as to minimize the error between the process and reference.

Assumes the knowledge of the plant dynamic model and set point performances is minimized.

$$J(\theta) = \frac{1}{2} e^2 \tag{3.14}$$

The most sense, to adjust the parameters in the set point of J's negative gradient in order to execute J small, that is,

$$\frac{d\theta}{dt} = -\gamma \, \frac{\partial J}{\partial} = -\gamma \, e \, \frac{\partial e}{\partial \theta} \tag{3.15}$$

Where,   is the function of the optimization, is adaptation gain

The partial derivative, $\frac{\partial e}{\partial \theta}$ which is called the sensitivity derivative of the system, it tells how the error is influenced by the variable parameter. When it is assumed that the parameter variations are slower than other adjustable in the system, then the derivative, $\frac{\partial e}{\partial \theta}$ can be evaluated under the assumption that θ is constant.

$$G(s) = \frac{-40s + 26.8}{10800s^2 + 721s + 0.67}, G_m(s) = \frac{Ym(s)}{Uc(s)} = \frac{s + 10}{s^2 + 8s + 10}$$

The control law is given by:

$$U(t) = \theta 1 Uc(t) - \theta 2 Y(t) \quad (3.16)$$

Where,

U(t) is the control law, $\theta 1$ and $\theta 2$ are parameters of control, $Y(t)$ is the output of the system. Then, the Laplace transform form of control law is written as;

$$U(s) = \frac{Y(s)}{G(s)} = \theta 1 Uc(s) - \theta 2 Y(s)$$

$Y\frac{10800s^2+721s+26.8}{-40s+0.67} = \theta 1 Uc(s) - \theta 2 Y(s)$, from this, $\frac{Y(s)}{U_c(s)} = \frac{-40s+26.8}{10800s^2+(721+\theta 2)s+\theta 2+0.67}$

$$e = Y - Ym \quad (3.17)$$

$$E(s) = Y(S) - Ym(s)$$

Where,

The error between the output of the reference model and the real system is indicated by e(t).

$\frac{Y(s)}{U_c(s)} = \frac{-40\theta_1 + 26.8\theta_1}{10800s^2 + (721+\theta_2)s + \theta_2 + 0.67}$, but, $G_m(s) = \frac{Y_m(s)}{U_c(s)}$, $Ym(s) = Gm(s)Uc(s)$

The equation (3.33) will becomes:

$$e = \frac{-40\theta_1 + 26.8\theta_1}{10800s^2 + (721 + \theta_2)s + \theta_2 + 0.67} U_c - \frac{s + 10}{s^2 + 8s + 1o} \quad (3.18)$$

$$\frac{\partial e}{\partial \theta_2} = \frac{-40s + 26.8}{10800s^2 + (721 + \theta_2)s + \theta_2 + 0.67} = G_m(s)U_c(s) \quad (3.19)$$

$$\frac{\partial e}{\partial \theta_2} = \frac{-\theta_1(40s + 26.8)(40s + 26.8)}{[10800s^2 + (721 + \theta_2)s + \theta_2 + 0.67]^2} U_c(s) = \frac{Y^2(s)}{\theta_1 U_c(s)} \quad (3.20)$$

3.5.1 Stability of the Plant

To analyze the stability of the plant can be describe by transfer function is $G(s)\frac{-40s+26.8}{10800s^2+721s+0.67}$.

This plant stability analyze can be done using quadratic formula and Routh Hurwitz Criterion. In this thesis I choose Routh Hurwitz Criterion to analyze the stability of plant, in this case it will be as following. The typical equation $10800s^2 + 721s + 0.67$

The Concept Routh Array:

Row	**First column**	**Second column**
S^2	10800	0.67
S^1	721	0
S^0	0.67	

Calculation of S^0 row:$b_2 = \frac{721\times0.67-10800\times0}{721} = \frac{483.07}{721} = 0.67$

The complete Routh array is:

$$\begin{array}{c|cc} s^2 & 10800 & 0.67 \\ s^1 & 721 & 0 \\ s^0 & 0.67 & \end{array}$$

Poles: S_1 = -0.0095 and S_2 = -0.0658

Zeros: S = 0.67

The Routh- Hurwitz Criterion: there is no sign change in the first column, this Complying stability.

Therefore, the system described by transfer function $G(s) = \frac{-40s+26.8}{10800s^2+721s+0.67}$ is stable.

3.6 Simulink Model of a SISO System Reference Model

Figure 3.2 shows the SISO system of reference model's Simulink model.

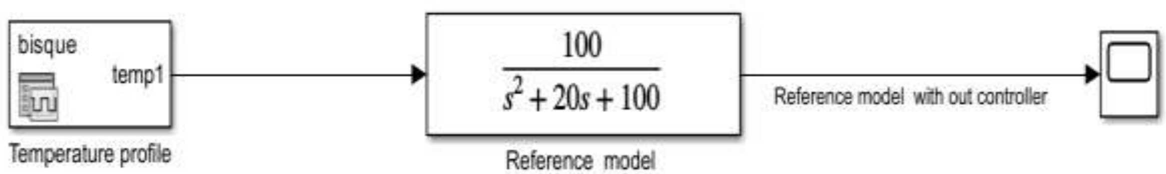

Figure 3.2: Simulink Model of reference model

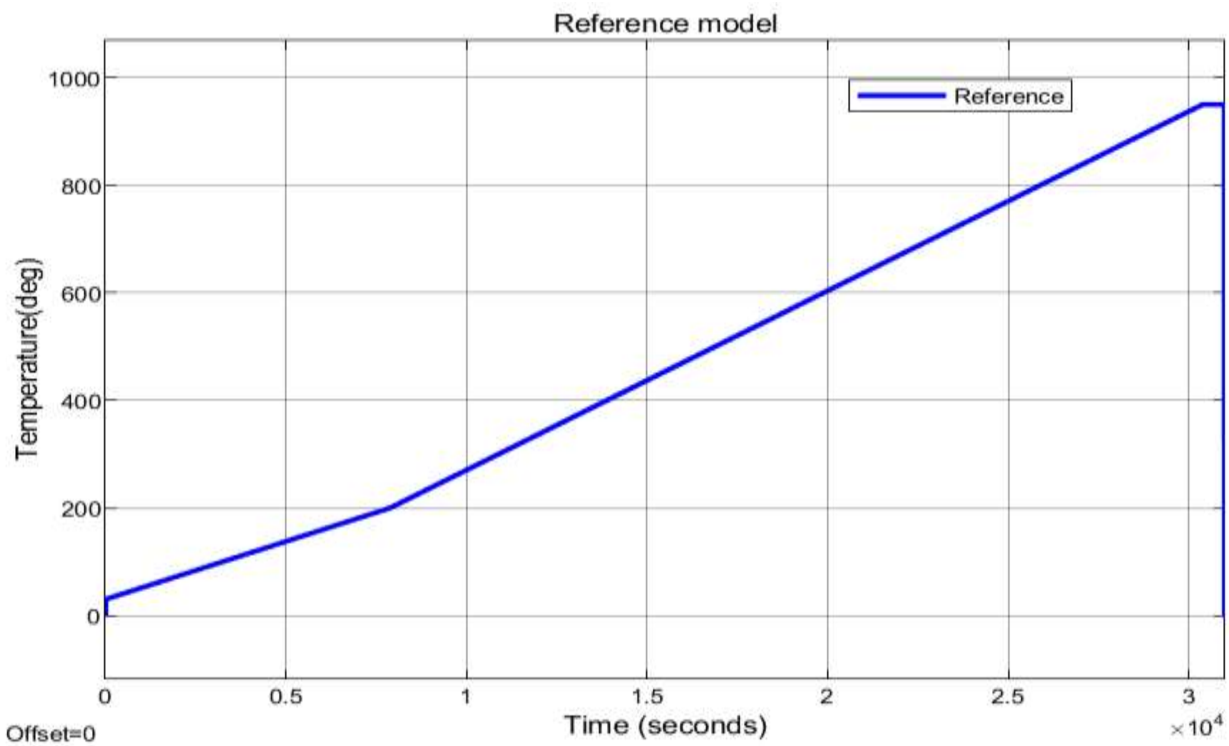

Figure 3.3: Simulation Result of reference Model

3.7 Simulink Model of an Electrical kiln (Plant)

Figure 3.4 shows the Simulink model of the SISO structure of the plant without a controller.

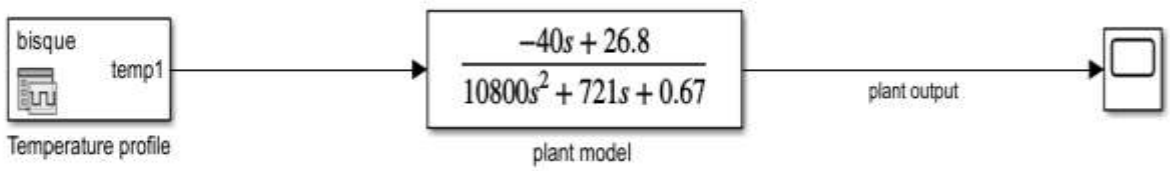

Figure 3.4: Simulation model SISO system of the plant model without controller

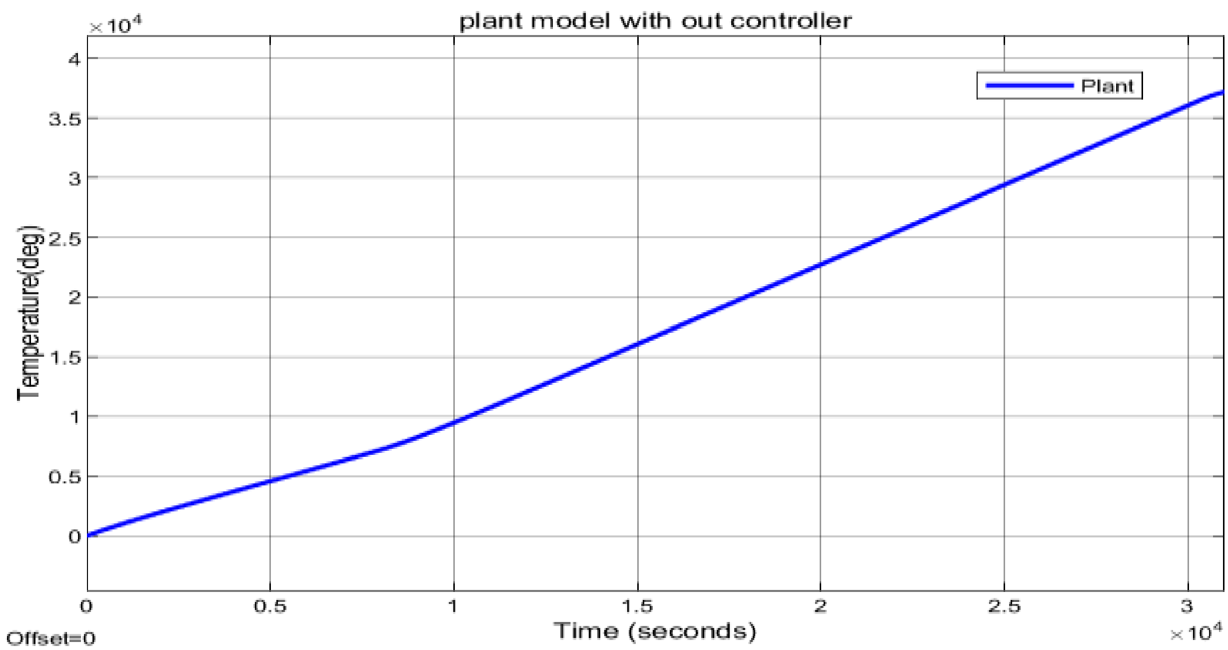

Figure 3.5: Simulation result of plant model without controller

The open loop response of SISO system is shown figure 3.5. The response is continuously increased which means does not get settled for desired value temperature of clay firing process. Thereby, there is the need of closed loop system with a controller for control the value at the desired value and settle the output.

Form the above simulation result we can analyze the temperature profile response of Reference Model output and Plant output using in the following Table

Table 3.1 Performance comparison of plant and reference model

Criteria	Plant and reference Model	
	Plant Model without controller	Reference Model without Controller
Rise Time	23349	23349
Settling Time	29438	28245
Settling minimum	32360	810
Settling maximum	35953	950
Overshoot (%)	0.0144	0
Undershoot	0	0
Peak	35900	950
Peak Time	32400	28805

CHAPTER FOUR

CONTROLLER DESIGN AND ANALYSIS

4.1 Controller Design for an Electrical kiln

In this research, three temperature control strategies PID, Fuzzy Logic Controller (FLC), and Model Predictive Control (MPC) are developed and analyzed to regulate the temperature profile of an electric clay kiln used in Ethiopia's traditional pottery sector. The goal is to achieve precise tracking of the kiln's firing stages, which include bisque firing, and glaze firing. Each controller is designed to enhance system stability, minimize energy usage, and effectively handle the kiln's nonlinear characteristics and inherent time delays.

4.2 PID Controller

In the industry process control, a popular of the process control loops are based on Proportional-Integral-Derivative (PID) controllers that have been at the heart of control engineering fields. Fundamentally PID controllers are categories into two types of , these are conventional PID's and advance PID's (robust, gain scheduling, intelligent, soft computing - fuzzy, neuro fuzzy -neuro, fuzzy neuro-genetic).PID controllers are utilized in most automatic processes and control applications in industry to control flow, temperature, pressure, level and other industrial process variables[36]. Owing to its transparency, practicability, and capacity to broadly meet performance standards, the PID algorithm is frequently used in classical controllers. Consequently, PID control may eliminate study-state error and still accounts for over 80% of the total. Parameter setting interferes with PID control's performance and has a lot of limitations for control systems with complicated object models that are hard to figure out. PID control may not be able to meet technical standards for short adjustment periods and minimal overshoot due to the inconsistent speed and overshoot[37]. Proportional-Integral- Derivative (PID) controllers, among other practical feedback controllers, are extensively used in a variety of control applications. Before taking appropriate action to reduce the process error as much as possible, a PID controller looks at the error between its input process variable and that target value since its main goal is to keep the process as close as possible to the desired set point while minimizing the error. Based on the total number of faults, error conversion rate, and current errors, actions are done [38].

4.2.1 Algorithm of PID Controller

An error value is the difference between a desired set point and a measured process variable that is continuously analyzed by a PID controller. Through the adjustment of a control variable, the controller makes an ongoing effort to lower the error. The mathematical model for a proportional, differential, and integral control, or PID controller, is as follows [37]:

$$U(t) \;=\; Kp[e(t) + \frac{1}{Ti}\int_{o}^{t} e\,(t)dt + Td\,\frac{d\,e(t)}{dt}] \tag{4.1}$$

Where $u\,(t)$ is the controller's output, $e\,(t)$ is the deviation signal, which is the difference between the input value and the output value of the control object that the controller receives as input, Kp is the controller's scaling coefficient, K_i is its integration time, and K_d is its differential time. It is also possible to parametrize the controller as:

$$U(t) \;=\; K(e(t) + \frac{1}{\tau i}\int_{0}^{t} e\,(\tau)d\tau + \;\tau d\,\frac{de(t)}{dt}) \tag{4.2}$$

In this case, the terms "integral time" τ_i and "derivative time" τ_d. The derivative can be thought of as a prediction of future errors based on linear extrapolation, the integral as an average of past errors, and the proportional portion acting on the error's present magnitude. The process variable (PV) that the PID controller produces is the average of its three corrective terms, which include proportional, integral, and derivative.

$$PV(t) \;=\; Pout \;+\; Dout \tag{4.3}$$

4.2.2 PID Controller Parameters

The three standard parameters of PID controllers are proportional, integral, and derivatives terms; each of these terms serves a particular purpose in the control process.

The purpose of the proportional term (P), is to drive the error in the direction of minimization, allow the control effect to occur as quickly as feasible, and provide a timely reaction to the current error[39]. Changes the dynamic performance and steady-state error will be disrupted by this term. The steady-state error (SSE) is inversely related to proportional gain and proportionate to process gain. SSE can be reduced by including an integral term to the set point or output that acts as a compensating unfairness term, or it can be dynamically changed [40].

The proportional term is given by

$$Pout = K\, e(t) \quad (4.4)$$

Integral Term (I): This term's application aims to minimize steady state error while expediting the process of reaching the reference value. Any changes made to this term will affect the stability of the system and the steady state error[39]. The integral term's contribution varies with the degree and duration of the inaccuracy. The accumulate balance that needs to be rectified beforehand is provided by the integral in a PID controller, which is the total of the instantaneous errors over time. After that, the integral gain is multiplied by the accumulated error and added to the controller output.

The integral term is given by

$$I_{out} = Ki\int(\tau)d\tau \quad (4.5)$$

Derivative Term (D): This term is used to improve system stability and dynamic reaction speed. It can also predict future error variations, allowing for the introduction of an adjusted signal into the system before the error becomes too significant [39].

Determining the slop of error with time and multiplying this degree of change by the derived gain yields the derivative of process error. The derivative gain,K_d is the degree to which the derivative term contributes to the overall control action. PID controllers are widely applicable since they rely just on measured process variables rather than feature process knowledge. Explicit process needs can be handled by a PID controller by adjusting the three model parameters. The controller's response can be characterized by how quickly it reacts to errors, how much the system overshoots its set point, and how much any oscillation occurs in the system. The stability of the system is not guaranteed by the PID controller algorithm, nor even optimal control. For many applications, the appropriate system control may only be provided by utilizing one or two terms. The other settings are set to zero in order to do this. PI controllers are widely used because, although the derivative achievement is susceptible to measurement noise, the system may still be unable to reach its intended value if an integral term is missing.

Figure 4.1 depicts the PID controller's construction.

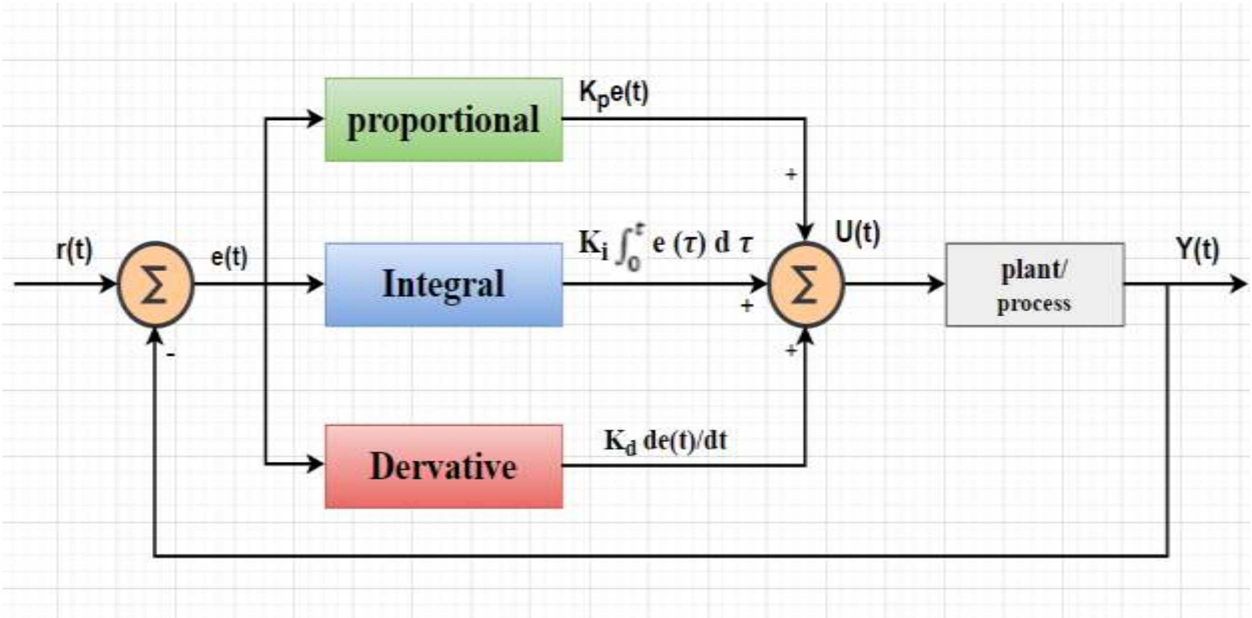

Figure 4.1: PID control structure [41]

Where, (t) and (t) indicate the system's error and control signals. K_p, K_i and K_d are proportional, integral, and derivative gain value consistently.

The transfer function of the PID controller $Gc\ (s)$ extra or alternative formula is provided by:

$$Gc(s) = Kp + \frac{Ki}{S} + Kds \tag{4.6}$$

4.2.3 Characteristics of P, I and D controllers

The Proportional (K_p) term -providing an overall control action proportional to the errors signal through the all- pass gain issue. The integral (K_i) term – minimizing stead state error through low frequency compensation by an integrator. The derivative (K_d) term-improving transient response through the high -frequency compensation by differentiator.

The individual effects of these three terms on the close -loop performance is concluded in the table 4.1. Note that this table helps a first guide for stable open-loop plants only. For optimum performance, K_p, K_i or T_i and K_d or T_d mutually dependent tuning.

Table 4.1 Effect of independent P, I and D

Closed-Loop Response	Rising Time	Overshoot	Setting Time	Steady-State Error	Stability
Increasing Kp	Decrease	Increase	Small Increase	Decrease	Degrade
Increasing Ki	Small Decrease	Increase	Increase	Large Increase	Degrade
Increasing Kd	Small Decrease	Decrease	Decrease	Minor Change	Improve

4.2.4 Limitation of PID controller

PID controller is can use for the several application industrial process control such as, level, pressure and temperature and others. However, because of its conventionality or simplicity, itis unable to manage the dynamics of non-linearity in the thermal regulation of an electrical heater utilized in the firing of clay. These are PID controller might struggle to handle nonlinearities effectively, as they trust on linear models and may not contain details of system, PID controller might has lack of adaptability needed for quickly change operating condition or disturbances, the tuning process can be time-consuming and might need adjustments when the system operating condition change, PID controller may lack of robustness in handling uncertainty.

4.3 MPC Controller

Model predictive control (MPC) is an advanced controls technique that has been utilized for process control since the 1980s. With the expanding computing power of chip (microcontroller), utilize of MPC has spread to real-time embedded applications, frequently utilized within the car and aerospace industries. MPC can has multi-input multi- output (MIMO) systems with coupled input-output channels, which streamlines the engineering of the control circle or loop [42].

The name MPC stems from the idea of utilizing an express model of the plant to be controlled which is utilized to predict the future output behavior. This prediction capability permits understanding optimal control issues on line, where tracking error, to be specific the deference between the predicted output and the specified reference, is minimized over a future horizon, possibly subject to limitations on the controlled inputs, outputs and states[43].

MPC is a model-based controller, in MPC Kalman filter utilized to forecast the process parameter of the whole process. For forecasting the future situation of the controller, MPC is used. The general aspect of model control for prediction is to gauge future manipulated variable trajectory U to improve the characteristics of plant output Y in future [44]. The requirements of MPC are include linear and nonlinear system, multi-input-multi-output system, system with delay, constrained system and hybrid systems. Unlike most control algorithms, MPC has the ability to forecast the future response of plant. At each control interval, MPC attempts to establish future plant behavior by means of an online optimizations process, which maximizes the tracking performance under certain constrains [45].

4.3.1 MPC Optimization

The easiest way to apply the MPC control rule is to see Figure (4.2). For any anticipated combination of current and upcoming control modifications $\Delta(k)$, $\Delta U(k + 1)$, $\Delta U(k + M - 1)$, the vector ΔU is frequently referred to as the choice variable in the optimization literature. Since the development of predictive control, the problem has been solved within the parameters of retreating horizon control, being cautious of each horizon window's restrictions. It gives us a way to solve the limited control problem analytically and permits us to modify the limits at the start of each window optimization. The outcome of the system's future behavior $(\boldsymbol{k} + \mathbf{1}/\boldsymbol{k})$, $(\boldsymbol{k} + \mathbf{2}/\boldsymbol{k})$. . . $(\boldsymbol{k} + \boldsymbol{p}/\boldsymbol{k})$, Predicting above the ($P$ = 20) prediction horizon is possible. The control horizon or changes are shown by (m = 4), as is ($\boldsymbol{M} \leq \boldsymbol{P}$). To calculate the best controlled output system (i.e., the output that follows a reference trajectory as best it can). In order to minimize object functions, J, the modified variables, (k), $at\ the\ K^{-th}$ sample instance are determined. As displayed in the form that follows[46]:

$$J = \sum_{I=1}^{p} ||\Gamma^{y}\iota\left[Y\left(K + \frac{1}{K}\right) - r\left(K + \frac{1}{K}\right)\right]||^{2} + \sum_{I=1}^{p} ||r^{u}\iota[Y(K + 1 - 1)]||^{2} \tag{4.7}$$

Where, $\Gamma^{y}\iota$ and $\Gamma^{u}\iota$ are weighting matrices used to penalize input and output signal components, respectively, at a predetermined future period.

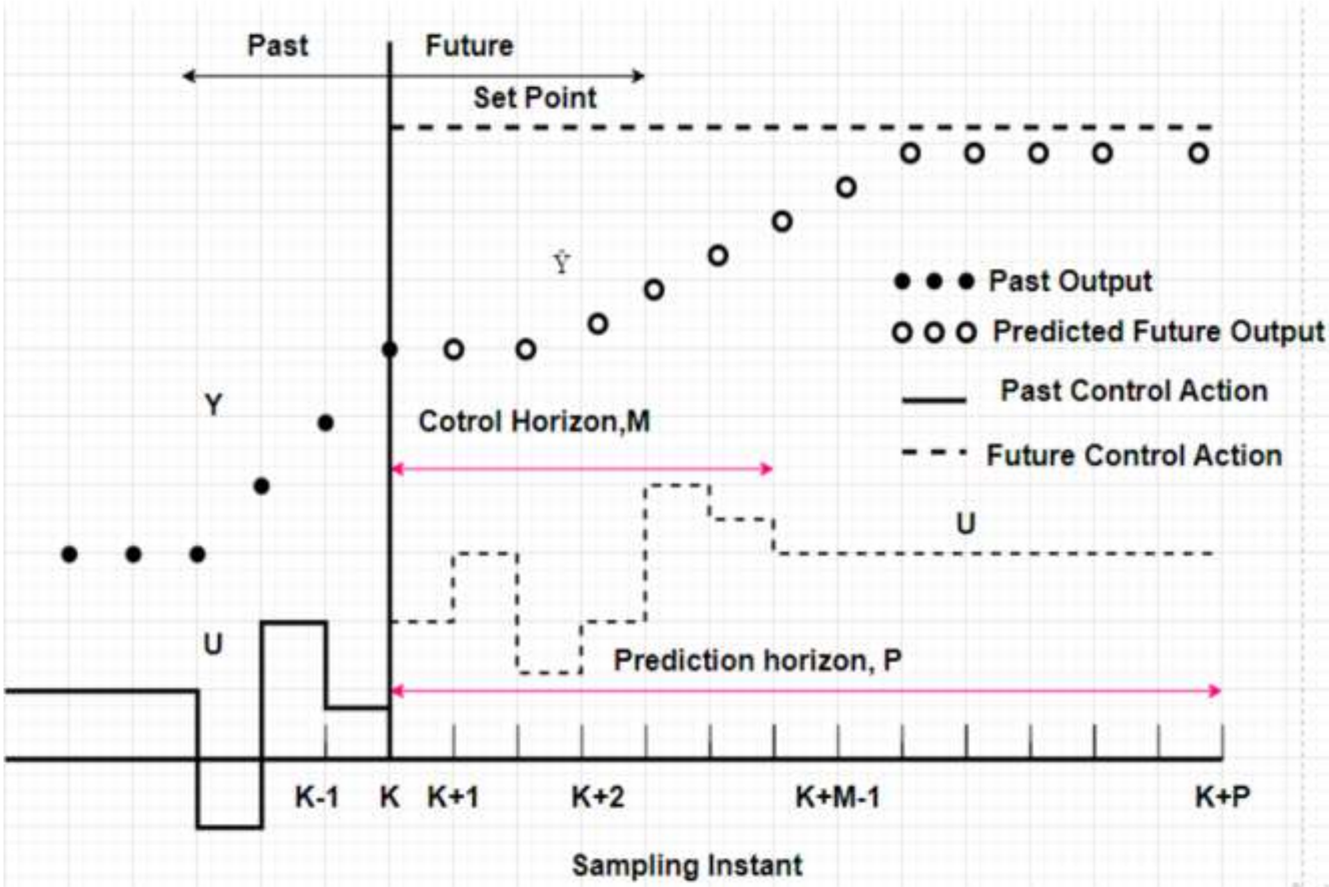

Figure 4.2: Model Predictive Controller [46]

4.3.2 MPC Calculation

The control calculations are based on the future projections and current measurements as indicated in the figure (4.2). The calculations are as follow:

1. The values of the manipulated variables, $\boldsymbol{u}$,, at the subsequent sampling instants at the K^{-th} sampling instant, $\{\boldsymbol{u}(k), \boldsymbol{u}\ (k + 1), \ldots, \boldsymbol{u}(k + m - 1)\}$ are calculated. The objective of calculating this set of $\boldsymbol{M}$'$\boldsymbol{s}$ is to satisfy the limitations and minimize the predicted deviations from the reference trajectory over the following P sampling instants.
2. Next, u(k), the initial control motion, is put into practice.
3. The first control moves, $(k + 1)$, is implemented at the next sampling time, $k + 1$, and the $M - step$ control policy is recalculated for the next M sampling instants, $k + 1$ to $k + m$.
4. Next, for the subsequence sampling instant, repeat steps 1 and 2.

4.3.3 MPC Structure

We create the following diagram to show the basic MPC structure in order to integrate the retreating horizon control idea into the plant. It is clear from the figure that a process model is used by the MPC controller throughout the whole control process for predicting the plant's future outputs depending on inputs and starting values. In order to obtain optimal future inputs that are to be transmitted to the plant, the optimizer with cost function and limitations also takes control effort and future errors between expected output and reference trajectory into considerations. The plant's output will then be submitted back to the process model as its current value to start the following predicted horizon [39].

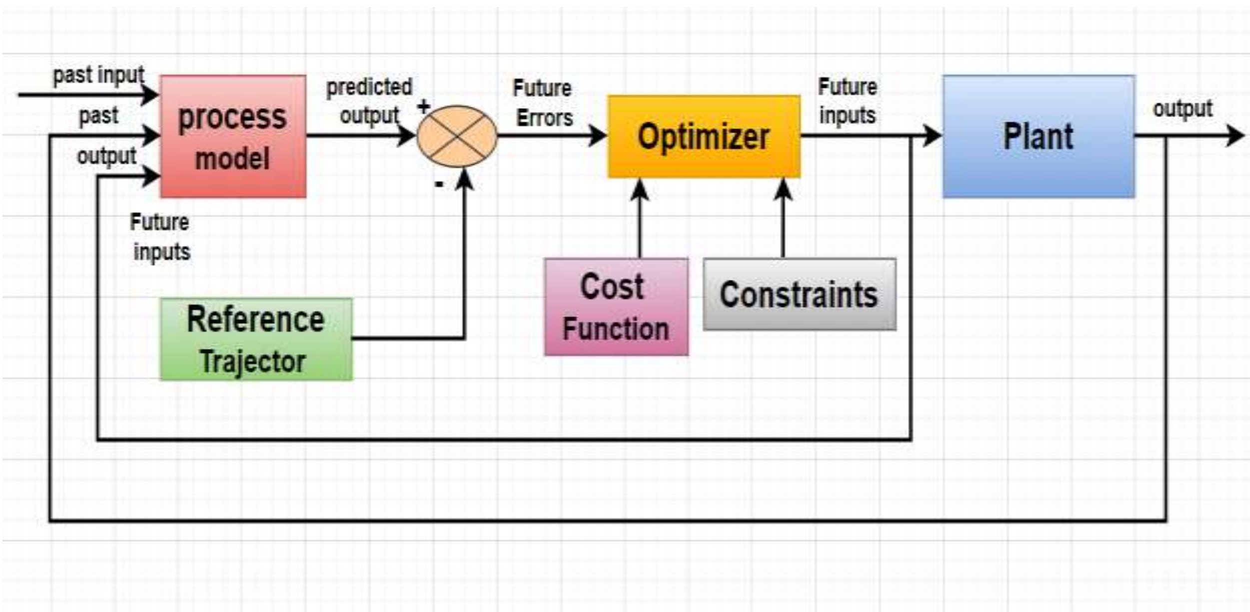

Figure 4.3: Structure of model predictive controller [39]

4.4 The Dynamic Model of Model Predictive Control

MPC is used in many industrial applications where greater durability and performance are required. The cost function provided by is minimized to provide the control signal[47].

$$J = \sum_{k=1}^{ny} e^T(k)Q(k)e(k) + \sum_{k=0}^{nu-1} u^T(k)R(k)u(k) \qquad (4.8)$$

The discrete -time state-space model is given as:

$$x(k + 1) = Ax(k) + Bu(k) \tag{4.9}$$

$$y(k) = Cx(k) + Du(k) \tag{4.10}$$

Where $e(K)^{\text{l}} * 1 - r(K)^{\text{l}} * 1$ is error, $y(K)^{\text{l}} * 1$ is system output, $r(K)^{\text{l}} * 1$ is system reference, $u(K)^{\text{l}} * 1$ is system input, $Q(K)^{\text{l}} * 1 \ and \ R(K)_{m*m}$ are weighting matrices, $X(K)_{n*1}$ is system states, $A_{n*n}, B_{n*m}, C_{\text{l}*n}, D_{\text{l}*m}$ are parameters of the system, m is number of inputs, $^{\text{l}}$ is number of outputs, n is number of states, n_y is prediction horizon value and nu is control horizon value.

Over the prediction horizon n_y, the model's recursive form is provided by:

$$\hat{x}(K+1) = P_x X(K) + H_x \hat{u}(K) \tag{4.11}$$

Where,

$$\hat{x}(K+1) = \begin{bmatrix} x(K+1) \\ x(K+2) \\ x(K+3) \\ . \\ . \\ . \\ x(K+ny) \end{bmatrix}, \hat{u}(K) = \begin{bmatrix} u(K) \\ u(K+1) \\ u(K+2) \\ . \\ . \\ . \\ u(K+ny-1) \end{bmatrix}, p_x = \begin{bmatrix} A \\ A^2 \\ A^3 \\ . \\ . \\ . \\ A^{ny} \end{bmatrix},$$

$$H_x = \begin{bmatrix} A & 0 & 0 & \cdots \\ AB & B & 0 & \cdots \\ A^2B & AB & B & . \\ . & . & . & . \\ . & . & . & . \\ A^{ny^{-1}}B & A^{ny^{-2}}B & A^{ny^{-3}}B & . \\ & & & \end{bmatrix}$$

$$\hat{Y}(K+1) = \begin{bmatrix} y(k+1) \\ y(k+2) \\ y(k+3) \\ . \\ . \\ . \\ y(k+ny) \end{bmatrix}, P = \begin{bmatrix} CA \\ CA^2 \\ CA^3 \\ . \\ . \\ . \\ CA^{ny} \end{bmatrix}, H = \begin{bmatrix} CB & 0 & 0 & \cdots \\ CAB & CB & 0 & \cdots \\ CA^2B & CAB & CB & \cdots \\ . & . & . & \cdots \\ . & . & . & \cdots \\ & . & & \\ CA^{ny^{-1}}B & CA^{ny^{-2}}B & CA^{ny^{-2}} & \cdots \end{bmatrix}$$

$\hat{x}(K+1)_{(n*n_y)*1}$ is the predicted system states, $\hat{u}(K)_{(m*n_y)*1}$ is input of the system, $\hat{y}(K+1)_{(l*n_y)*1}$ is the output of the system and

$P_{x(n*n_y)*n}, H_{x(n*n_y)*(m*n_y)}, P_{(n*n_y)*n}, H_{(n*n_y)*(m*n_y)}$ are parameter of the system over the prediction horizon n_y. The minimization of (1) with respect to (k) without considering the variable constraints is given by:

$$U(K)_{MPC} = L[(H^T \hat{Q}(K)H + H^{T^{\wedge T}}{}_{Q}(K)H + 2R^{T^{\wedge T}}(K))^{-1} 2H^{T^{\wedge}}{}_{Q}(K)(\hat{r}K) - P_x(K)] \quad (4.12)$$

Where,

$L_{m*(m*n_y)} = \left[I_{m*m:\ \ om*(m*n_y-m)}\right], I_{(m*m-m)}$ is matrix of an identity, $om*(m*n_y-m)$ is a zero matrix, $\hat{r}(K)_{(l*n_y)*1}$ is reference of the system, $\hat{Q}(K)_{(l*n_y)*(l*n_y)}$ and $\hat{R}(K)_{(m*nu-1)*(m*nu-1)}$ are weighting matrices. One of the primary functions of the MPC is thought to be the solution of the restricted optimization issue. Inputs, input rates, outputs, and output states can all be used to illustrate system limitations. The Illustrations of these include:

$$u\_(k) \leq u(k) \leq \bar{u}(k) \quad (4.13)$$

$$\Delta u\_(k) \leq \Delta u(k) \leq \Delta\bar{u}(k) \quad (4.14)$$

$$y\_(k) \leq y(k) \leq \bar{y}(k) \quad (4.15)$$

$$x\_(k) \leq x(k) \leq \bar{x}(k) \quad (4.16)$$

The state and output constraints can be typically expressed as extra constraints for the input in the loop since the outputs, (k) and (k), are functions of the control input, (k).

$$W(k)u(K) \leq f(k) \quad (4.17)$$

Where, in accordance with constraints number $n_c, f(K)_{nc+1}$ and $W(K)_{nc*m}$ represent the system constraints parameter. Compared to other approaches, the softening constraints method has a reduced computing overhead among the constraint handling techniques. This method incorporates the violation of the input signal's limitations into the cost function, resulting in:

$$J = \sum_{k=1}^{ny} e^T(k)Q(k)e(k) + \sum_{k=0}^{ny-1} u^T(k)R(k)u(k) + \sum_{k=0}^{ny-1} (W(k)u(k) -$$

$$f(k))^T s(k)(W(K)u(k) - f(k)) \quad (4.18)$$

Where,$S(K)_{m*m}$ weighting matrix. Considering maximum input constraint:

$$U(k) \leq \bar{u}(k)m * 1 \quad (4.19)$$

Then,

$$f = \bar{u}(k) and\, W(K) = I,$$

Where, the upper limit of the control signal is denoted by $\bar{u}(k)m * 1$. The following gives the control signal that minimizes the function (4.18) is given as:

$$U(K)_{MPC} = L[(H^T \hat{_Q}(K)H + H^T Q^T(K)H + {_{2R}^{\wedge}}(K)2_S^{\wedge T}(K))^{-1}(2H^{T\wedge T}_{Q}(K)(\hat{_r}(K) - P_x(K) +$$

$$2_S^{\wedge T}(K)\bar{\bar{_u}}(K)] \quad (4.20)$$

The maximum limits of the control signal and weighting matrix across the control horizon $nu - 1$ are represented by $\bar{\bar{_u}}(K)_{(m*nu-1)*1}$ and $\hat{_S}(K)_{(m*nu-1)*(M*nu-1)}$. In order to penalize the states or control inputs, it is crucial for controller design to choose the weighting matrices $Q(k)$ and $R(k)$ correctly. Greater weighting values indicate a smaller set of variables. The best values for the weighting factors can be obtained by applying the design technique.

4.5 Fuzzy logic controller

Fuzzy logic is a branch of artificial intelligence that deals with reasoning algorithms used to emulate human thinking and decision making in machines. These algorithms are used in applications where process data cannot be represented in binary form. For example, the statements “the air feels cool” and “he is young” are not discrete statements. Fuzzy logic interprets vague statements like these so that they make logical sense. In the case of the cool air, a PLC with fuzzy logic capabilities would interpret both the level of coolness and its relationship to warmth to ascertain that “cool” means somewhere between hot and cold. In straight binary logic, hot would be one discrete value (e.g., logic 1) and cold would be the other (e.g., logic 0), leaving no value to represent a cool temperature [48].

In contrast to binary logic, fuzzy logic can be thought of as gray logic, which creates a way to express in-between data values. Fuzzy logic associates a grade, or level, with a data range, giving it a value of 1 at its maximum and 0 at its minimum [48-50].

Fuzzy logic requires knowledge in order to reason. This knowledge is provided by a person who knows the process or machine (the expert), is stored in the fuzzy system. For example, if the temperature rises in a temperature regulated batch system, the expert may say that the steam valve needs to be turned clockwise a "little bit." A fuzzy system may interpret this expression as a 10-degree clockwise rotation that closes the current valve opening by 5%. As the name implies, a description such as a "little bit" is a fuzzy description, meaning that it does't have a definite value.

Fuzzy logic has existed since the ancient times, when Aristotle developed the law of the excluded middle. In this law, Aristotle pointed out that the middle ground is lost in the art of logical reasoning; statements are either true or false. When PLCs were developed, their discrete logic was based on the ancient reasoning techniques. Thus, inputs and outputs could belong to only one set (i.e., ON or OFF); all other values were excluded. Fuzzy logic breaks the law of the excluded middle in PLCs by allowing elements to belong to more than just one set.

4.5.1 Fuzzy Sets

Define a universe of discourse, X, as a collection of objects all having the same characteristics. The individual elements in the universe X will be denoted as x. In classical, or crisp, sets the transition for an element in the universe between membership and non-membership in a given set is abrupt and well-defined (said to be ''crisp''). For an element in a universe that contains fuzzy sets, this transition can be gradual. This transition among various degrees of membership can be lead to the fact that the boundaries of the fuzzy sets are vague and ambiguous[48-50].

Hence, membership of an element from the universe in this set is measured by a function that attempts to describe vagueness and ambiguity. Elements of a fuzzy set are mapped to a universe of membership values (degree to which a quality is possessed) using a function-theoretic form in the range of [0, 1]. If an element in the universe, say x, is a member of fuzzy set A, then this mapping is given by $\mu(x) \in [0, 1]$[48].

4.5.3 Fuzzy Logic Control Components

The three main actions performed by a fuzzy logic controller are:

Fuzzification

Fuzzy processing

Defuzzification

As shown in Figure 4.5, when the fuzzy controller receives the input data, it translates it into a fuzzy form. This process is called fuzzification[48-50]. The controller then performs fuzzy processing, which involves the evaluation of the input information according to IF…THEN rules created by the user during the fuzzy control system's programming and design stages. Once the fuzzy controller finishes the rule-processing stage and arrives at an outcome conclusion, it begins the defuzzification process. In this final step, the fuzzy controller converts the output conclusions into "real" output data and sends this data to the process via an output module interface. If the fuzzy logic controller is located in the PLC rack and does not have a direct or built-in I/O interface with the process, then it will send the defuzzification output to the PLC memory location that maps the process's output interface module.

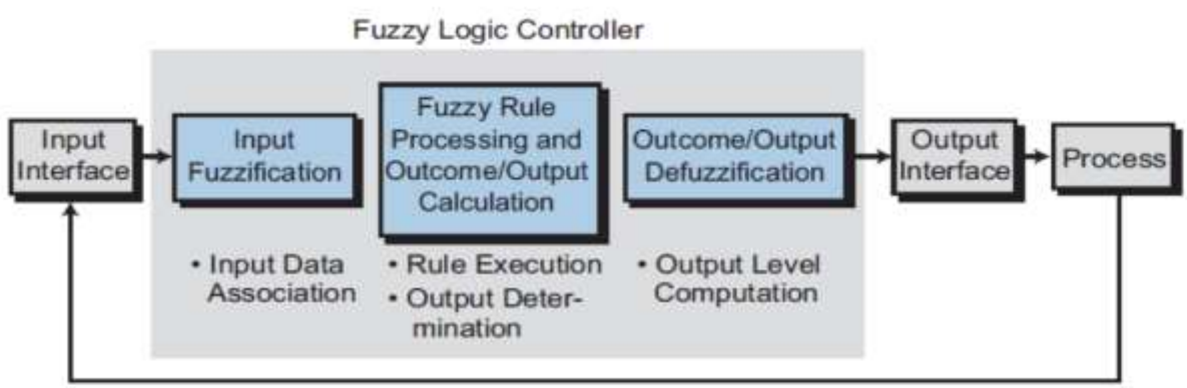

Figure 4.5: Fuzzy logic controller operations

FUZZIFICATION

Fuzzification is the process of making a crisp quantity fuzzy [48-49]. It transforms the physical values of the error signal, rate of change of error which is input to the fuzzy logic controller, into a fuzzy set consisting of an interval for the range of the input values and an associate membership function describing the degrees of the confidence of the input belonging to this range. The conversion process is performed by a membership function. The purpose of this fuzzification step is to make the input physical signal compatible with the fuzzy control rule base in the core of the controller. Fuzzification consists of two main components:

1. **Membership Functions:** During fuzzification, a fuzzy logic controller receives input data, also known as the fuzzy variable, and analyzes it according to user-defined charts called membership functions .Membership functions can have many shapes, depending on the data set, but the most common are the S, Z, and shapes shown in Figure (4.6). Note that these membership functions are made up of connecting line segments defined by the lines' end points. Each membership function can have up to three line segments with a maximum of four end points. The grade at each end point must have a value of 0 or 1.

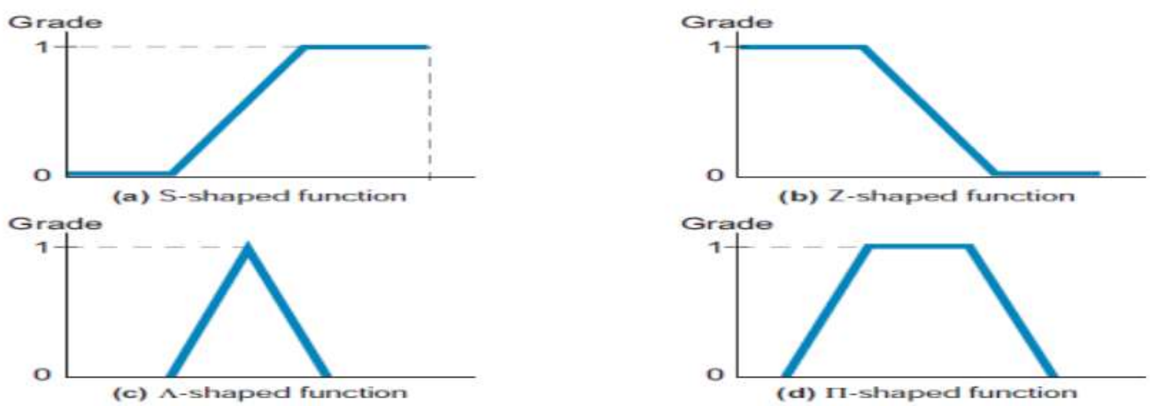

Figure 4.6: Membership function shapes (a) S, (b) Z, (c) Λ, and (d) Π.

2. **Labels:** Each fuzzy controller input can have several membership functions, with seven being the maximum and the norm that define its conditions. Each membership function is defined by a name called a label. For example, an input variable such as temperature might have five membership functions labeled as cold, cool, normal, warm, and hot. Generically, the seven membership functions have NL (negative large), NM (negative medium), NS (negative small), ZR (zero), PS (positive small), PM (positive medium) and PL (positive large) labels.

A group of membership functions forms a fuzzy set. Figure 4.7 shows a fuzzy set with five membership functions. Although most fuzzy sets have an odd number of labels, a set can also have an even number of labels. For example, a fuzzy set may have four or six labels in any shape, depending on how the inputs are defined in relationship to the membership function.

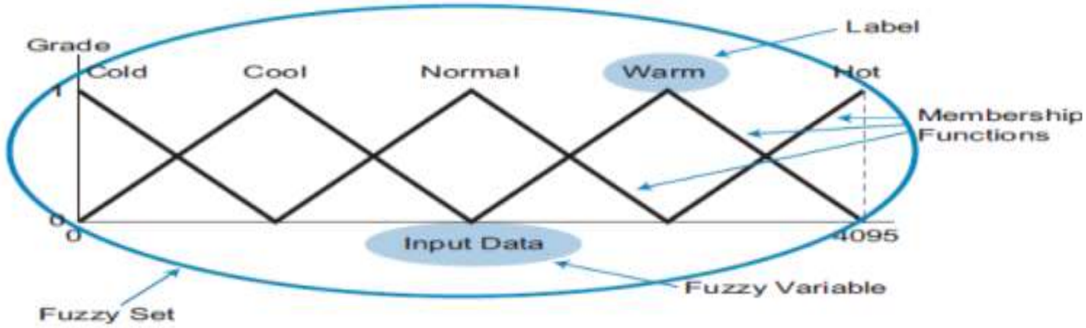

Figure 4.7: Fuzzy set with five membership functions

FUZZY PROCESSING COMPONENTS

During fuzzy processing, the controller analyzes the input data, as defined by the membership functions, to arrive at a control output. During this stage, the processor performs two actions

1. **Rule Evaluation:** Fuzzy logic is based on the concept that most complicated problems are formed by a collection of simple problems and can, therefore, be easily solved. Fuzzy logic uses a reasoning process composed of IF...THEN rules, each providing a response or outcome. Basically, a rule is activated, or triggered, if an input condition satisfies the IF part of the rule statement. This results in a control output based on the THEN part of the rule statement. Sometimes, more than one rule is triggered at a time in a fuzzy control process. In this case, the controller evaluates all the rules to arrive at a singleoutcome value and then proceeds to the defuzzification process. Fuzzy logic rules with two inputs are often represented in matrix form to represent AND conditions. For example, Figure 4.8 illustrates a 3 × 3 matrix (9 rules) that uses two inputs, X1 and X2, and one output Y1. One advantage of this matrix representation is that it makes it easy to represent all the rules for a system. A five-label system translates into a 5 × 5 matrix with 25 rules, while a seven-label system produces a 7 × 7 matrix with 49 rules. An even membership function combination (e.g., a system with 6 labels for one input and 4labels for another) will have a 24-rule matrix.

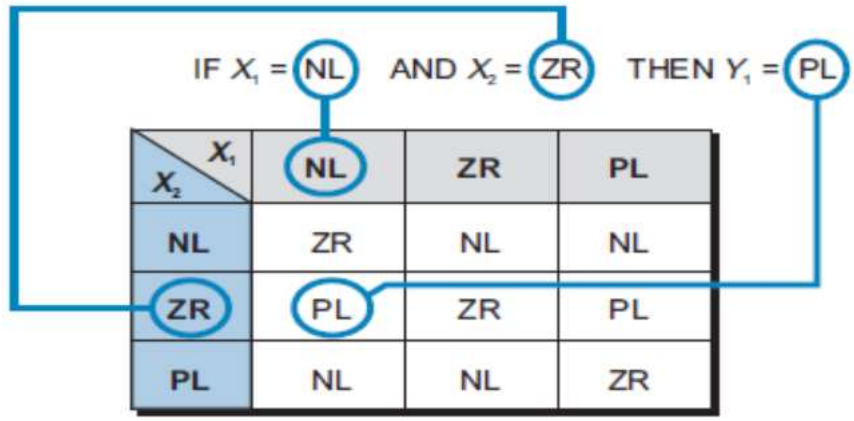

Figure 4.8: Fuzzy logic rule matrix.

2. **Fuzzy Outcome Calculations:** Once a rule is triggered, meaning that the input data belongs to a membership function that satisfies the rule's IF statement, the rule will generate an output outcome. This fuzzy output is composed of one or more membership functions (with labels), which have grades associated with them. The outcome's membership function grade is affected by the grade level of the input data in its input membership function. In Figure 4.9a, the fuzzy input FI of 60% belongs to two membership functions, ZR and PS, corresponding to the grades of 0.6 and 0.4, respectively. These two grades will have an impact on the amount of the output (see Figure (4.9)) by intersecting the output membership functions at the same grade levels (0.6 and 0.4). However, the output membership function that is selected for the final output value depends on the user's programming of the IF...THEN rules [48-49].

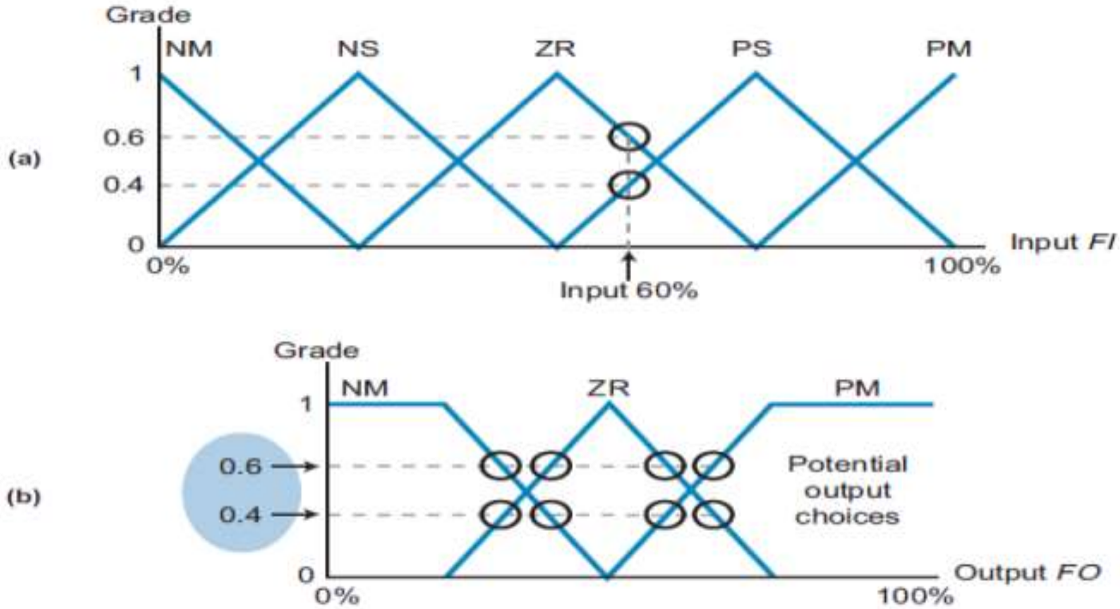

Figure 4.9: (a) Fuzzy input grades and (b) the resulting output grades.

The Inference Mechanism provides the mechanism for referring to the rule base such that the appropriate rules are fired. The two most commonly used inference procedures in FLC are Mamdani's Max-Min and Max-Algebraic Product (or Max-Dot) composition. The inference or firing with this fuzzy relation is performed via the operations between the fuzzified crisp input and the fuzzy relation representing the meaning of the overall set of rules. As a result of the composition, one obtains the fuzzy set describing the fuzzy value of the overall control output. In this thesis a Mamdani’s Max-min composition inference method is used [48-49].

DEFUZZIFICATION COMPONENTS

The final output value from the fuzzy controller depends on the defuzzification method used to compute the outcome values corresponding to each label. The defuzzification process examines all of the rule outcomes after they have been logically added and then computes a value thatwill be the final output of the fuzzy controller. The Fuzzy controller then sends this value to the output module. Thus, during defuzzification, the controller converts the fuzzy output into a real-life data value. There are many defuzzification methods, but all are based on mathematical algorithms. The two most common defuzzification methods are as follows:

1. **Maximum Value Method:** The maximum value method bases the final output value on the rule output with the highest membership function grade. This method is mainly used with discrete output membership functions.
2. **Center of Gravity Method**: The center of gravity method, also referred to as "calculating the centroid," mathematically obtains the center of mass of the triggered output membership functions. The center of gravity method is the most commonly used defuzzification method because it provides an accurate result based on the weighted values of several output membership functions. The center of gravity method applies to noncontinuous, or discrete, output membership functions, as well as continuous ones.

CHAPTER FIVE

SIMULATION RESULT AND DISCUSION

The electric clay kiln's mathematical modeling and the development of PID, fuzzy logic, and model predictive control techniques for controlling temperature profiles were covered in the previous chapters. The simulation results from the use of these controllers are presented and examined in this chapter.

5.1 Simulink model of a PID controller for Bisque Firing

In this study, the PID Tuner tool in MATLAB was employed to automatically determine optimal gains for the PID controller. Robustness here refers to the system's ability to maintain stable and accurate performance even when faced with considerable process uncertainties, such as variations in thermal dynamics.

Figure 5.1 presents the Simulink model of a closed-loop single-input single-output (SISO) electric kiln controlled by a PID controller. The plant is represented by the second-order transfer function incorporating a non-minimum phase characteristic, and the PID gains were automatically tuned to achieve robust performance against the observed initial inverse response and other disturbances.

This setup demonstrates how the tuned PID controller effectively handles the kiln's dynamics during bisque firing, ensuring reliable temperature regulation despite model uncertainties.

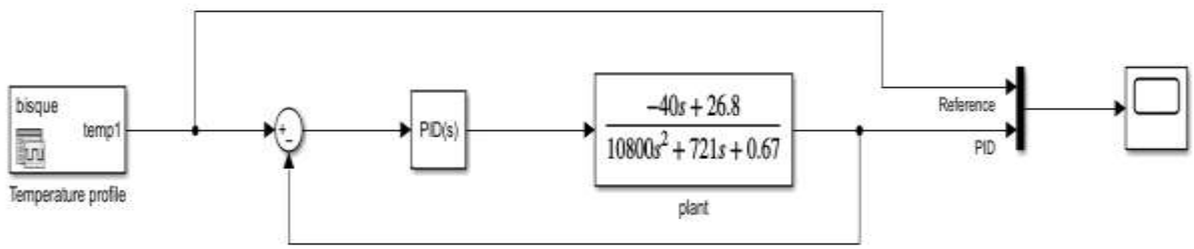

Figure 5.1: An electrical kiln with a Simulink-modeled of the PID controller for bisque firing

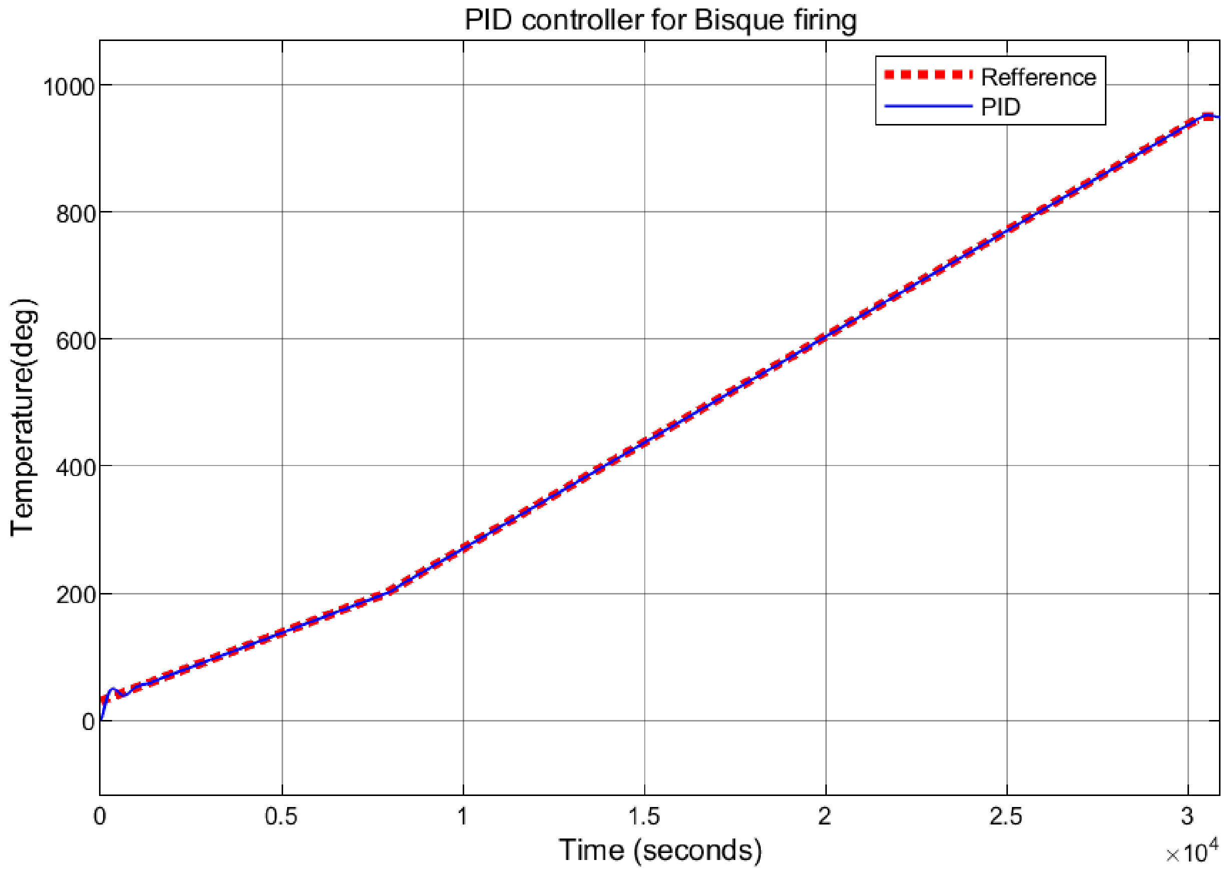

Figure 5.2: Temperature profile response of a PID controller for bisque firing

Figure 5.2 presents the closed-loop temperature profile response of the single-input single-output (SISO) system designed to control the temperature of an electric kiln during bisque firing. The simulation results demonstrate how effectively the PID controller manages the process dynamics.

Using MATLAB's PID Tuner, the controller gains were automatically optimized to P = 0.13754, I = 0.0019231, D = −0.38936, with a derivative filter coefficient N = 0.0357252.

5.2 Simulink model of MPC controller for Bisque Firing

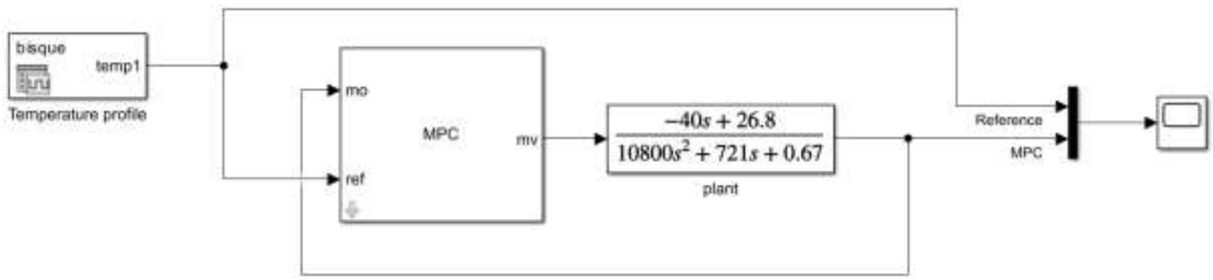

Figure 5.3: An electrical kiln with a Simulink-modeled of MPC controller for bisque firing

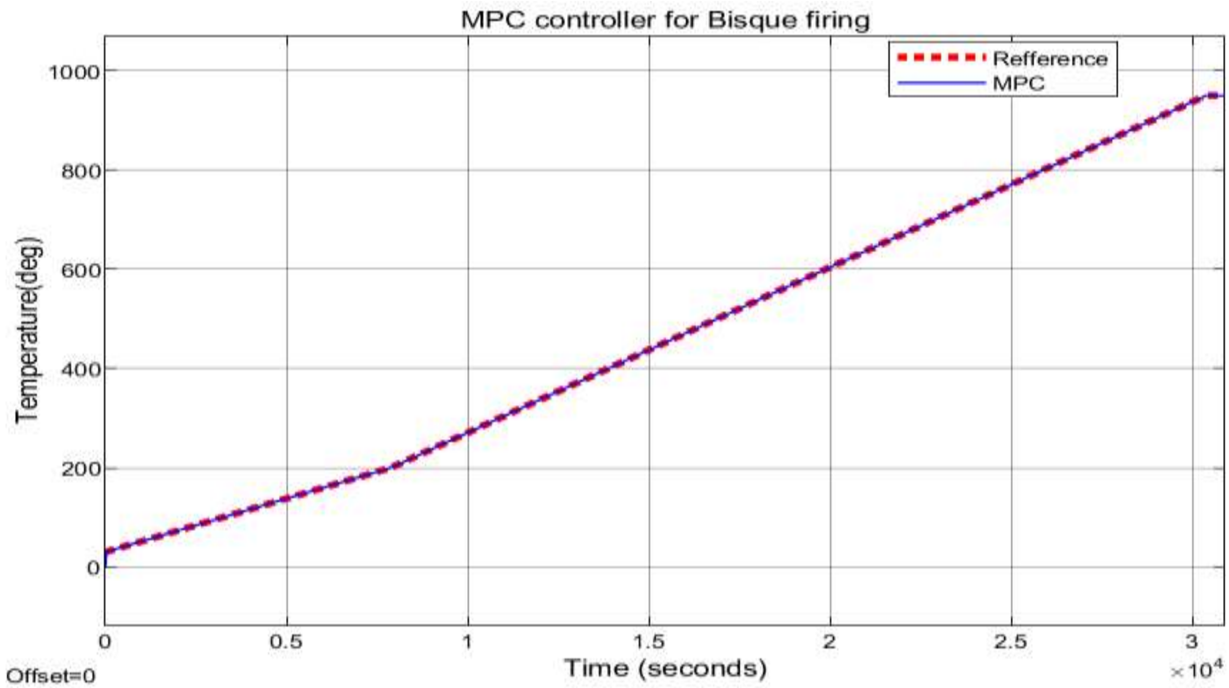

Figure 5.4: Temperature profile response of MPC controller for bisque firing

Figure 5.4 shows the closed-loop temperature profile response of the Model Predictive Control (MPC) system designed to regulate the temperature of an electric kiln during bisque firing. Building on the Simulink setup described earlier, this simulation highlights the MPC's impressive performance. With carefully configured parameters, the controller delivers exceptionally smooth and precise temperature tracking.

4.3 Fuzzy Logic Designer for Bisque Firing

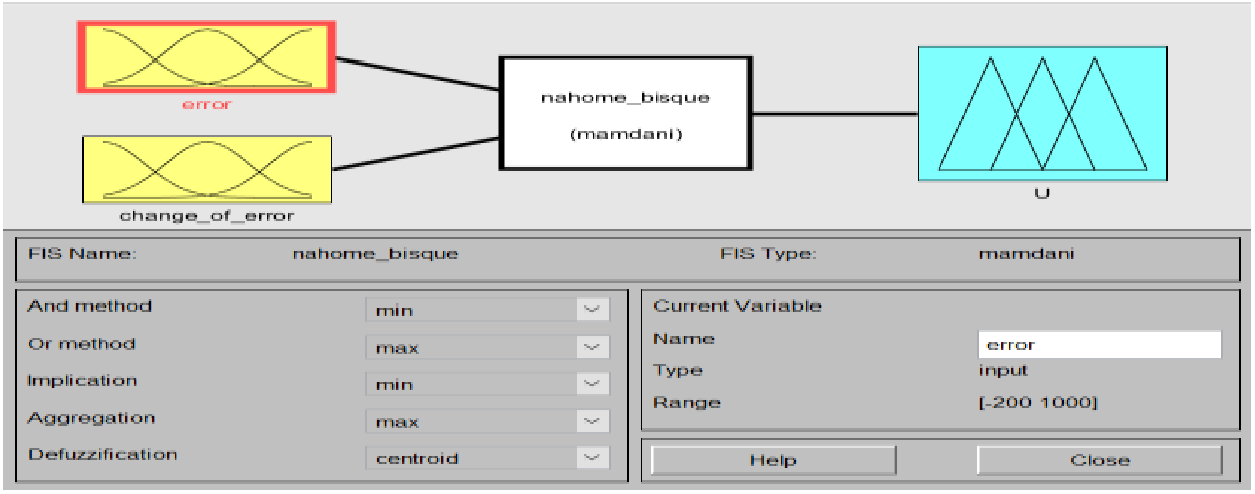

Figure 5.5: Fuzzy interface block

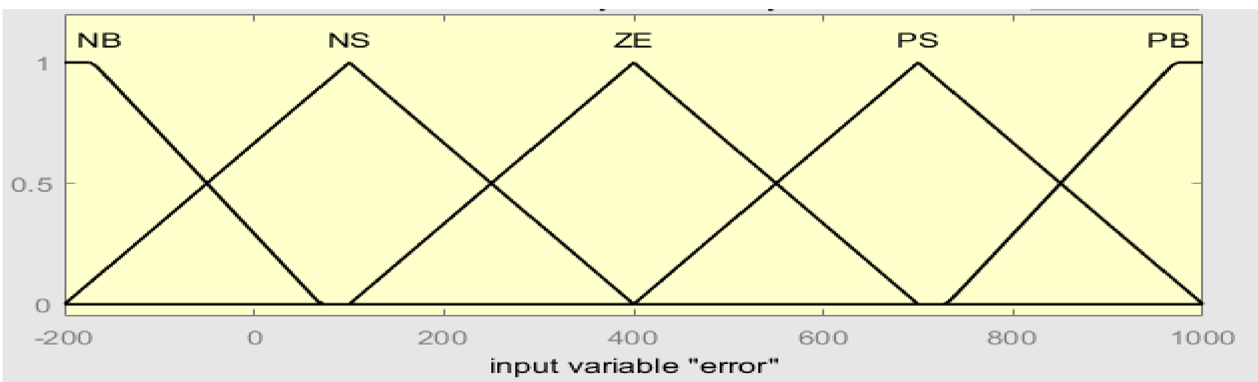

Figure 5.6: Input membership function for error

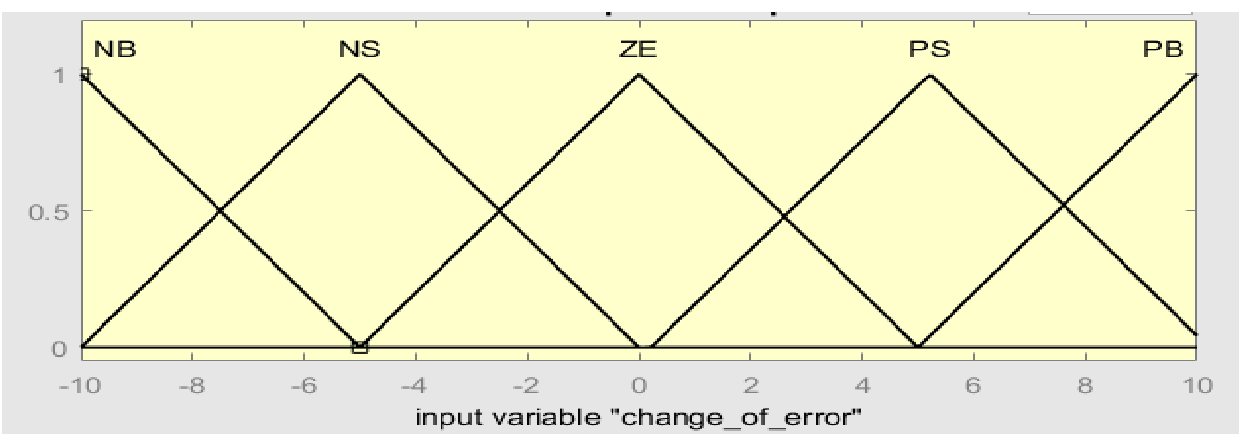

Figure 5.7: Input membership function for change of error

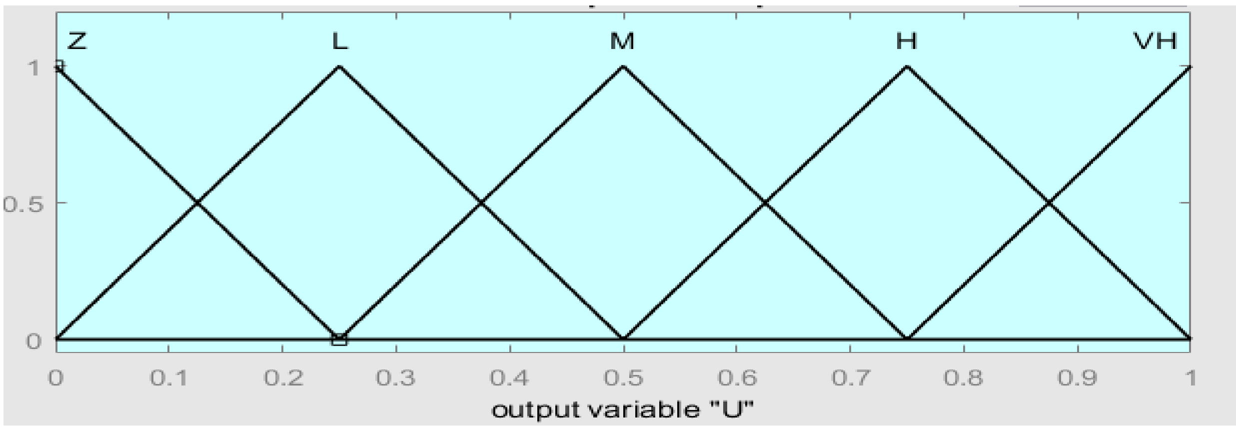

Figure 5.8: Output membership function for U (heater)

Table 5.2 Rule table for fuzzy logic designer

Error	**Change of error**				
	NB	**NM**	**ZE**	**PS**	**PB**
NB	Z	Z	L	L	M
NS	Z	L	L	M	H
ZE	L	L	M	H	H
PS	L	M	H	H	VH
PB	M	M	H	VH	VH

4.4 Simulink model of Fuzzy Logic controller for Bisque Firing

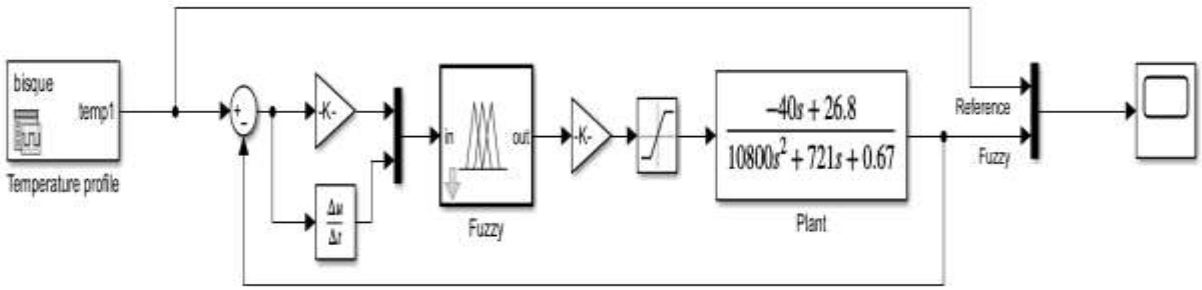

Figure 5.6: An electrical kiln with a Simulink-modeled of Fuzzy logic controller for bisque firing

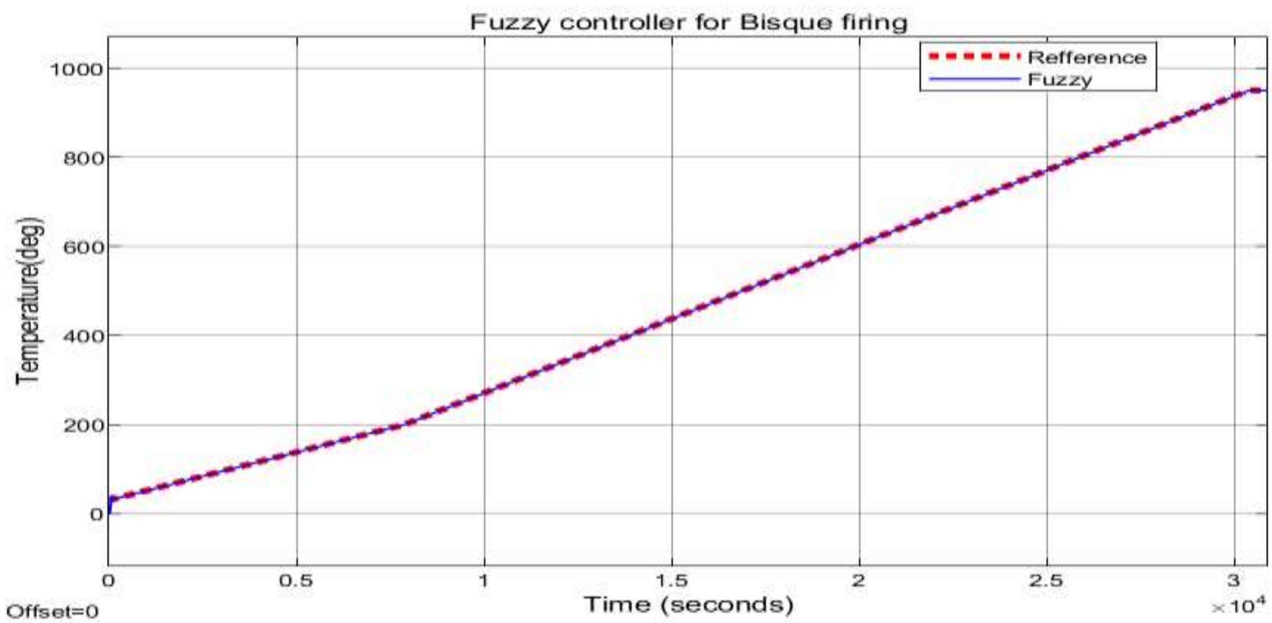

Figure 5.7: Temperature profile response of Fuzzy logic controller for bisque firing

Figure 5.6 presents the Temperature profile response of the Fuzzy Logic Controller (FLC) implemented for temperature control of the electric kiln during bisque firing.

5.5 Simulink model of PID, Fuzzy logic and MPC Controllers for bisque firing

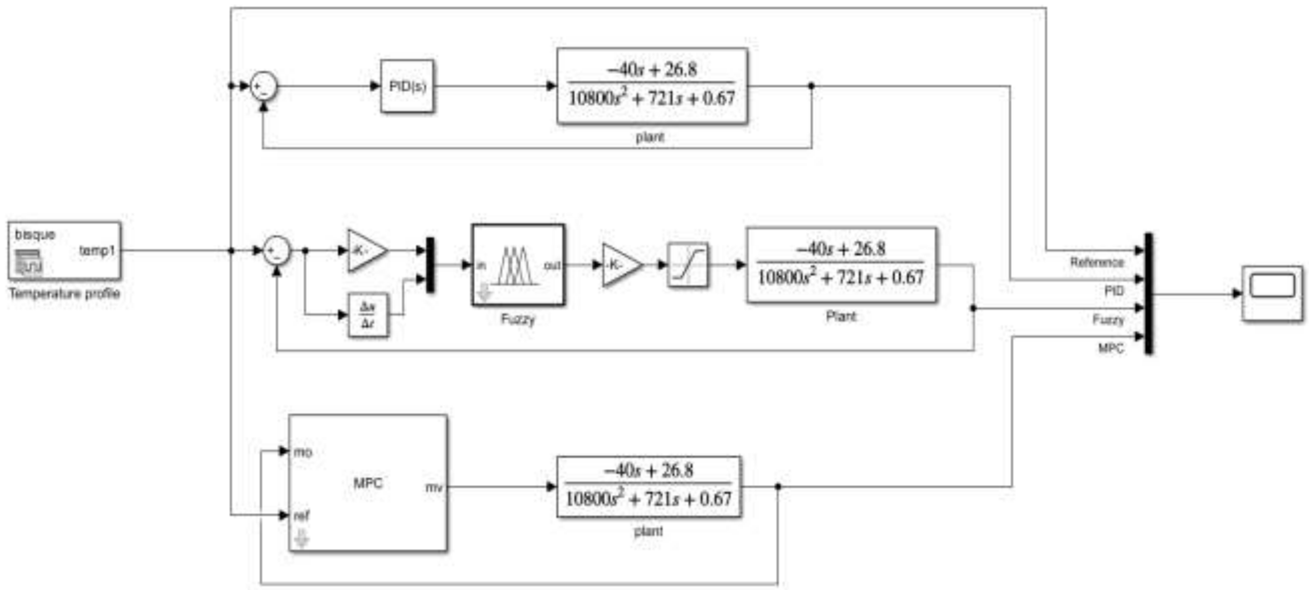

Figure 5.8: illustrates a Simulink model with PID, Fuzzy logic and MPC Controllers for bisque firing

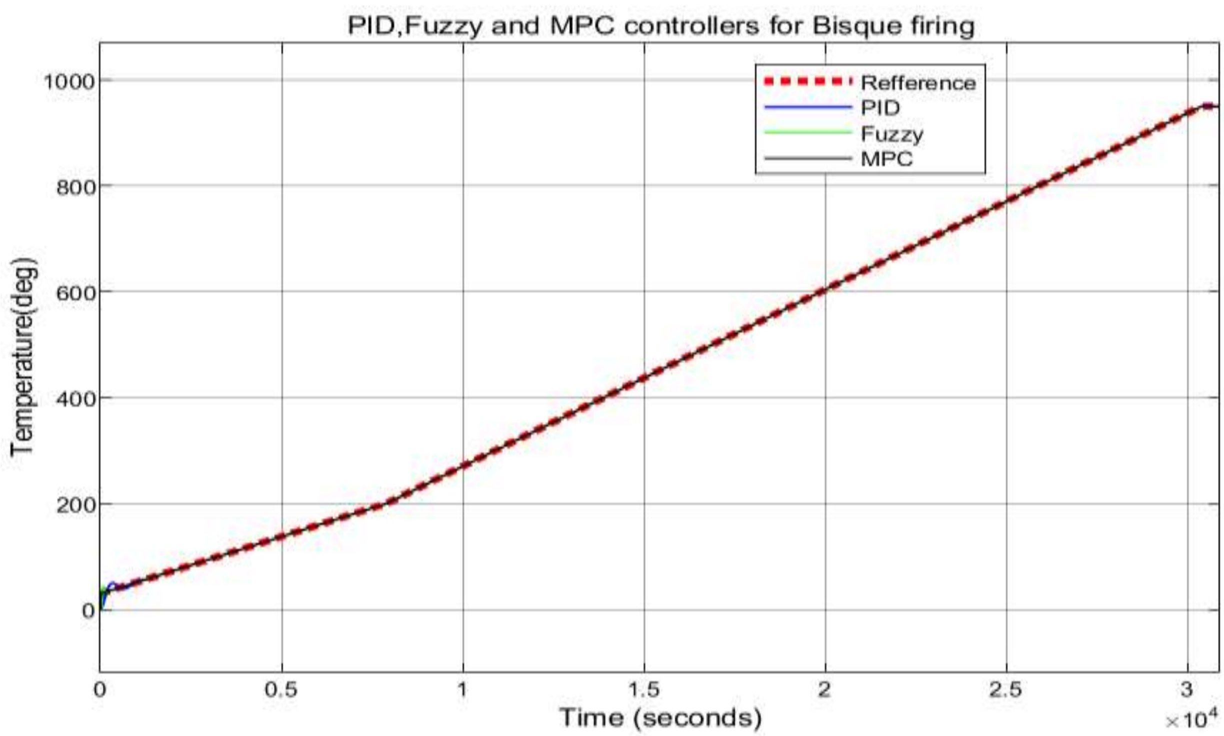

Figure 5.9: Temperature profile response of PID, Fuzzy logic and MPC Controllers for bisque firing

5.6 Temperature profile tracking performance for bisque firing

This section evaluates the performance of PID, fuzzy logic controller (FLC) and MPC for bisque firing temperature profile control. The assessment is based on standard profile performance metrics and energy efficiency indicators obtained from MATLAB/Simulink simulations.

Table 5.2 Performance Comparison PID, Fuzzy and MPC controllers for bisque firing

Criteria	PID Controller	Fuzzy logic Controller	MPC controller
IAE(^{o}c.s)	3.82 x 10^4	2.41 x 10^4	1.12 x 10^4
RMSE(^{o}c)	6.75	4.12	1.95
Max Error(^{o}c)	14.2	8.6	3.1
Overshoot %	2.1	0.6	0
Energy Index(kwh)	128.4	116.7	104.2
Power fluctuation	High	Medium	Low

Based on the performance comparison in Table 5.2, it is clear that the MPC controller is the most suitable and best-performing controller for the bisque firing process, followed by the Fuzzy Logic Controller, while the PID controller shows the weakest performance.

The PID controller exhibits the highest values of IAE, RMSE, and maximum error, which indicates poor tracking of the desired temperature profile during bisque firing. Although its overshoot is relatively small, the controller consumes the highest amount of energy (128.4 kWh) and shows high power fluctuation, which can cause thermal stress in the kiln and negatively affect the quality of ceramic ware. This makes PID less suitable for precise and energy-efficient bisque firing. The Fuzzy Logic Controller performs significantly better than PID. It reduces IAE, RMSE, and maximum error by a noticeable margin and limits overshoot to only 0.6%, resulting in smoother temperature tracking. Its medium power fluctuation and lower energy consumption (116.7 kWh) indicate improved stability and efficiency. This shows that fuzzy logic is well suited for handling the nonlinear and slow thermal dynamics of the kiln. The MPC controller clearly outperforms both PID and Fuzzy controllers across all performance metrics. It achieves the lowest IAE (1.12×10^4 °C·s), lowest RMSE (1.95 °C), and smallest maximum error (3.1 °C), demonstrating highly accurate temperature profile tracking. The zero overshoot is particularly important for bisque firing, as it prevents overheating and reduces the risk of cracking or deformation of clay products. In addition, MPC records the lowest energy index (104.2 kWh) and low power fluctuation, indicating superior energy efficiency and stable heater operation.

For the bisque firing process, where precise temperature control, minimal overshoot, and energy efficiency are critical, the MPC controller is the most effective and reliable solution. The Fuzzy Logic Controller is a strong alternative when MPC implementation complexity is a concern, while the PID controller is the least suitable due to its higher error, energy consumption, and power fluctuations.

5.6 Simulink model of PID controller for Glaze Firing

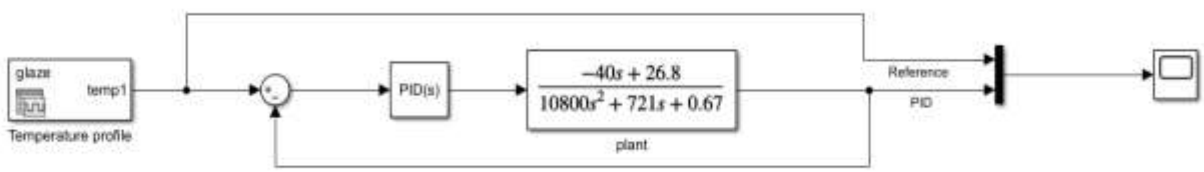

Figure 5.1: An electrical kiln with a Simulink-modeled of a PID controller for Glaze firing

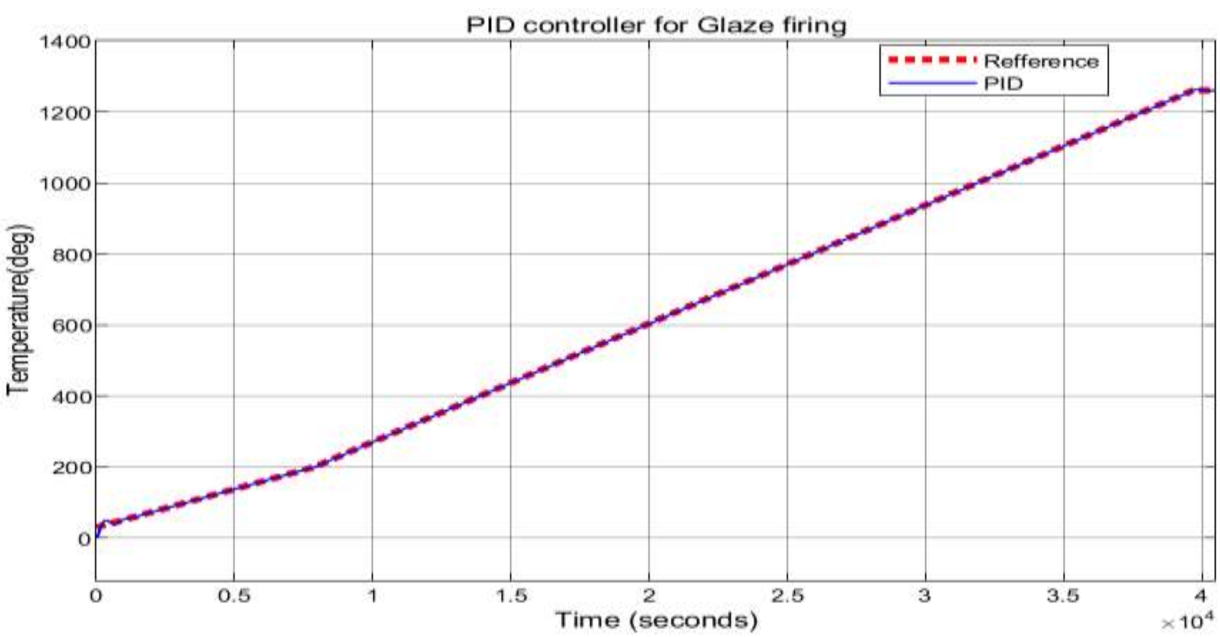

Figure 5.11: Temperature profile response of PID controller for Glaze firing

5.7 Simulink model of MPC controller for Glaze Firing

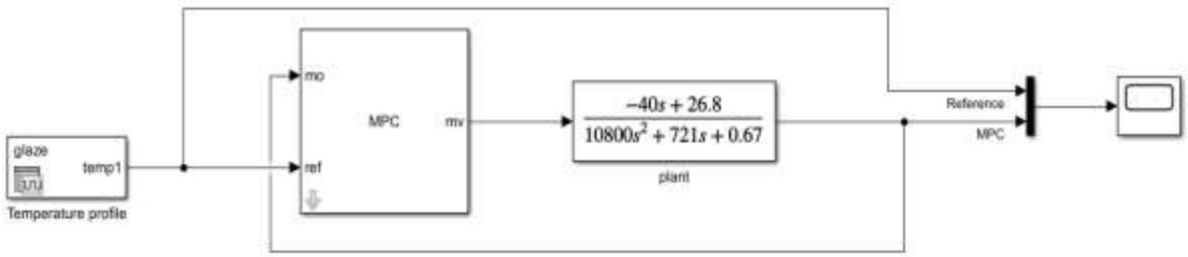

Figure 5.12: An electrical kiln with a Simulink-modeled of MPC controller for Glaze firing

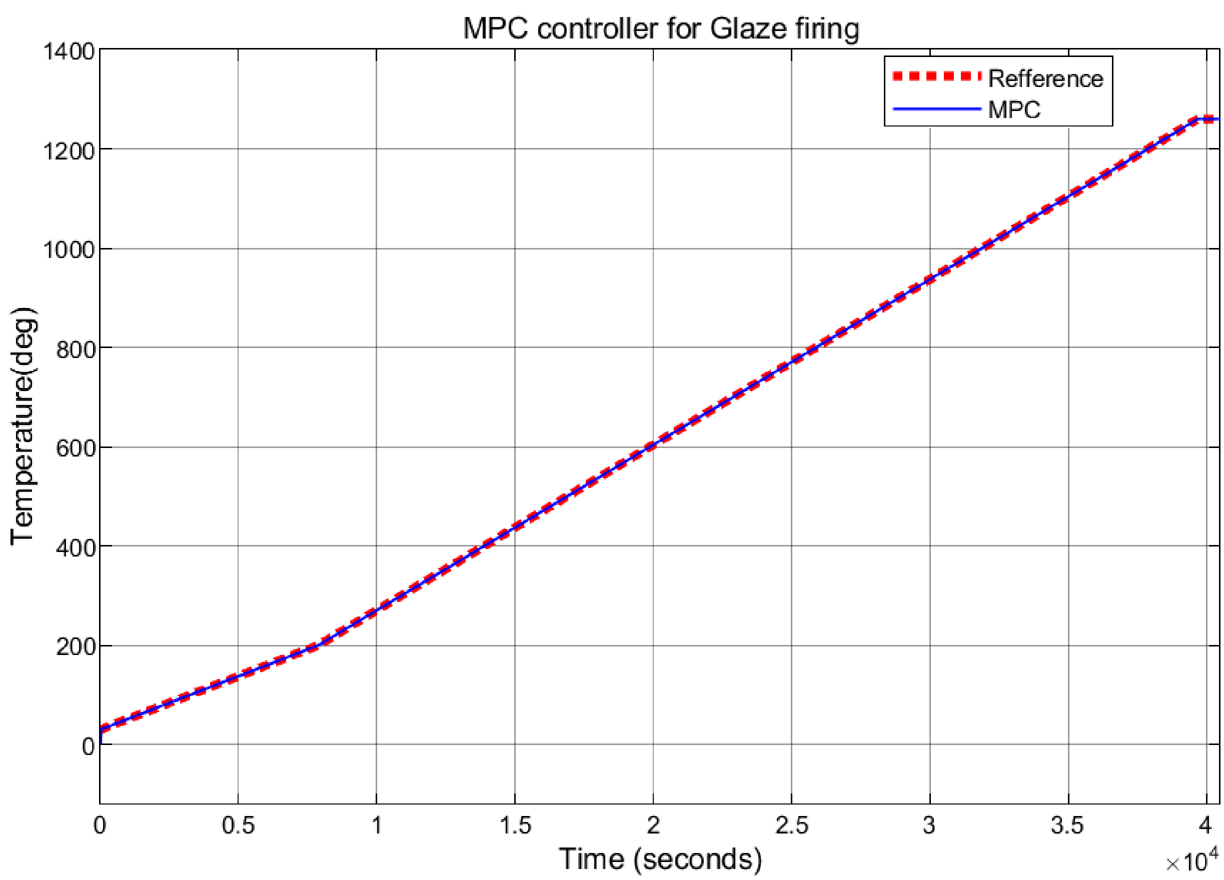

Figure 5.13: Temperature profile response of MPC controller for Glaze firing

5.8 Fuzzy Logic Designer for Glaze Firing

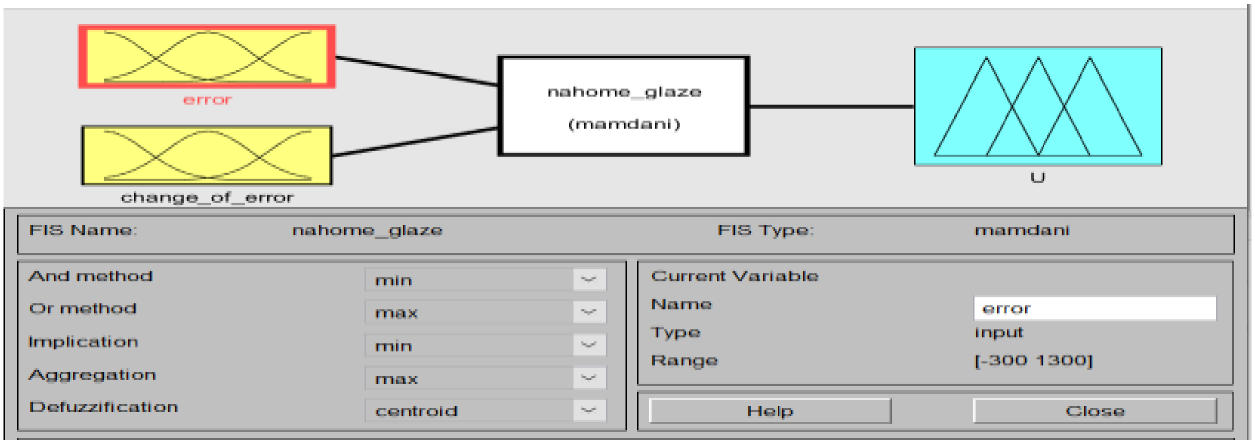

Figure 5.14: Fuzzy interface block

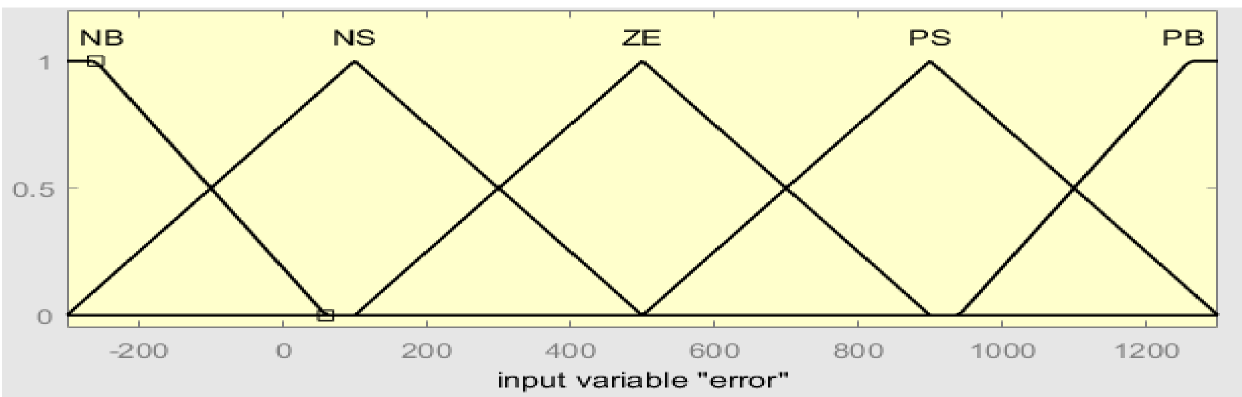

Figure 5.15: Input membership function for error

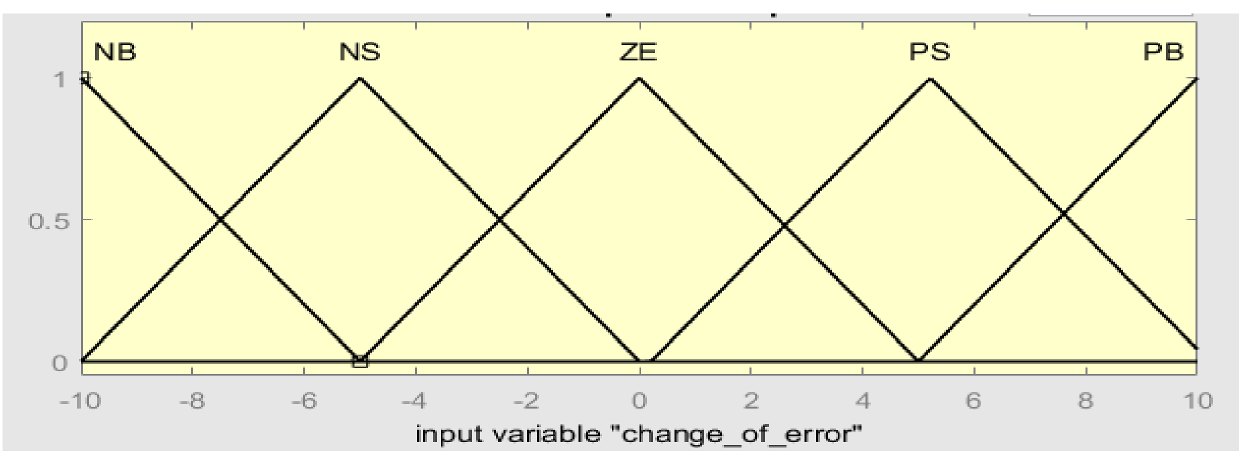

Figure 5.16: Input membership function for change of error

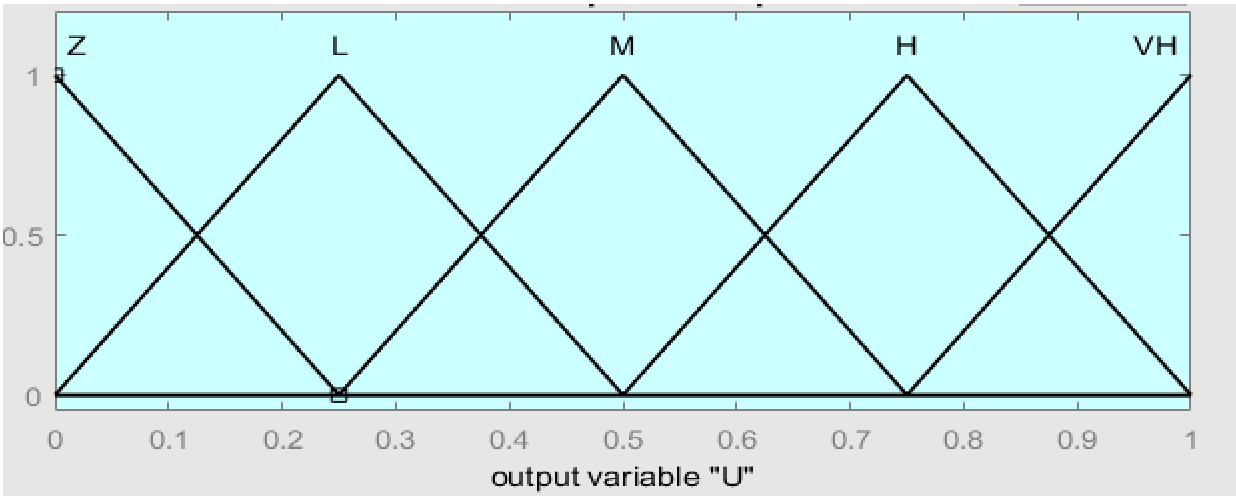

Figure 5.16: Output membership function for U (heater)

Table 5.3 Rule table for fuzzy logic designer for Glaze firing

Error	**Change of error**				
	NB	**NM**	**ZE**	**PS**	**PB**
NB	Z	Z	L	L	M
NS	Z	L	L	M	H
ZE	L	L	M	H	H
PS	L	M	H	H	VH
PB	M	M	H	VH	VH

5.9 Simulink model of Fuzzy Logic controller for Glaze Firing

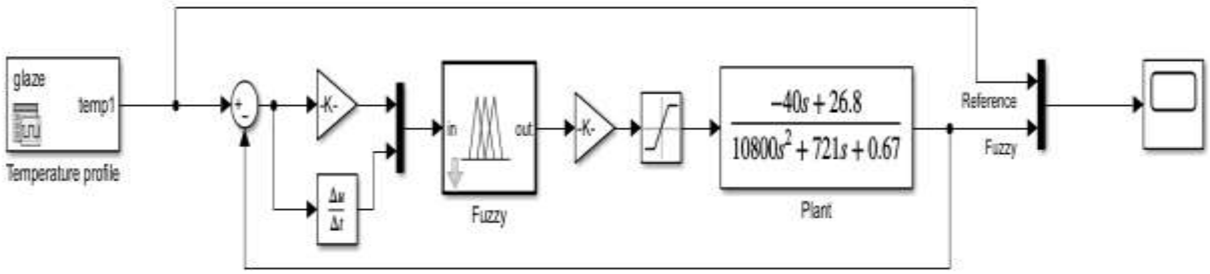

Figure 5.15: An electrical kiln with a Simulink-modeled of Fuzzy logic controller for Glaze firing

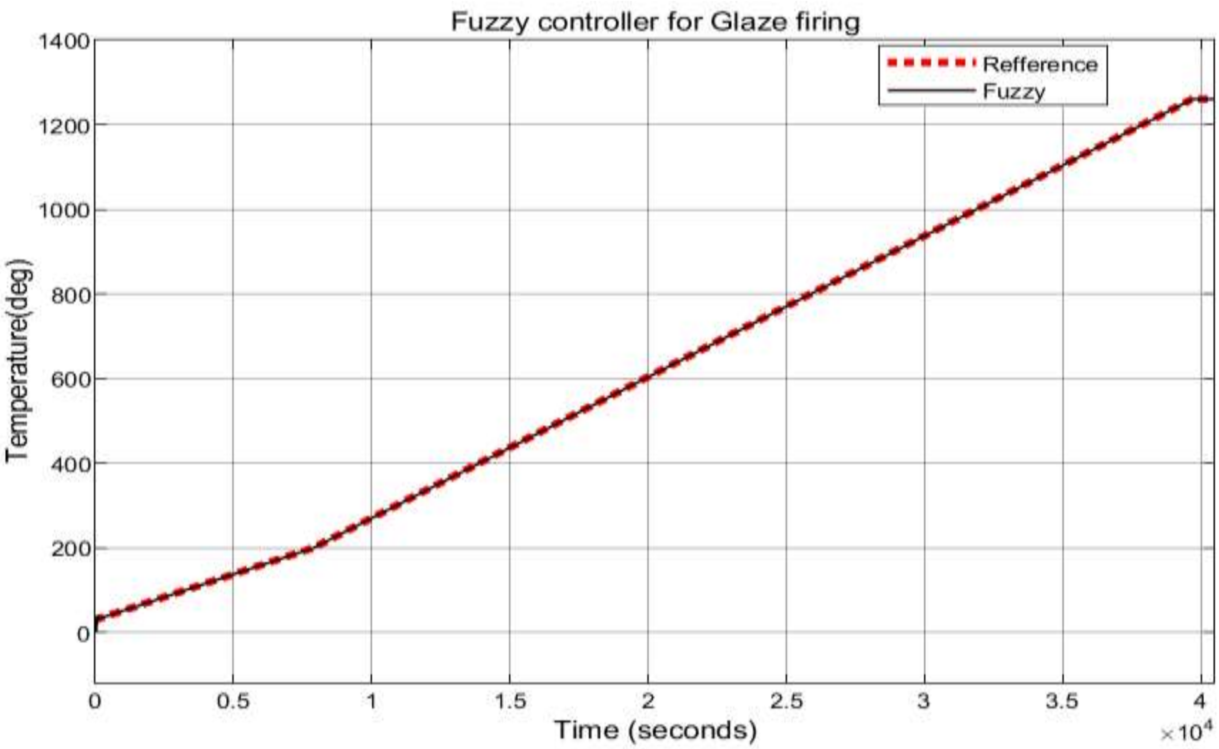

Figure 5.16: Temperature profile response of Fuzzy Logic controller for Glaze firing

5.10 Simulink model of PID, Fuzzy logic and MPC Controllers for Glaze firing

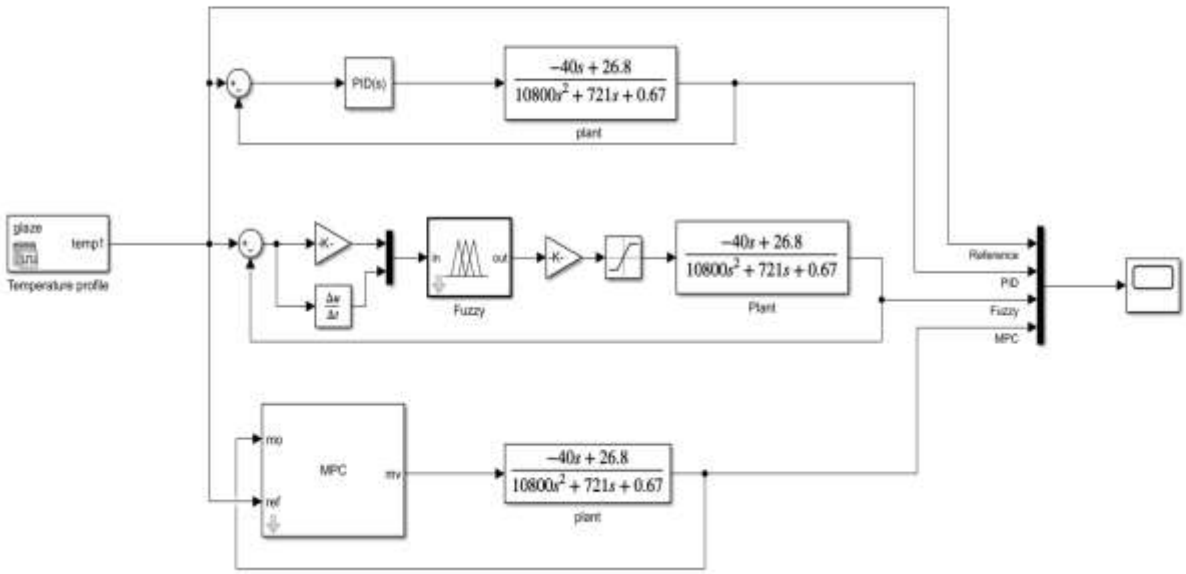

Figure 5.17: illustrates a Simulink model with PID, Fuzzy logic and MPC Controllers for Glaze firing

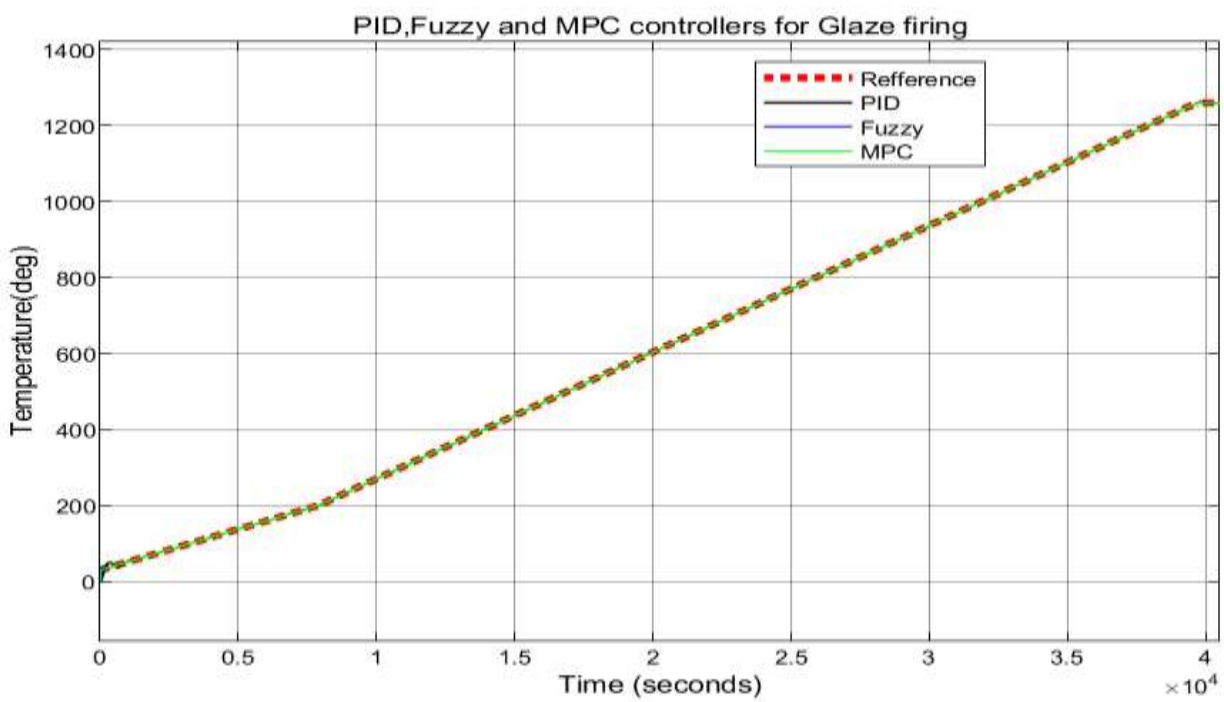

Figure 5.18: Temperature profile response of PID, Fuzzy logic and MPC Controllers for Glaze firing

5.11 Temperature profile tracking performance for Glaze firing

This section evaluates the performance of PID, fuzzy logic controller (FLC) and MPC for glaze firing temperature profile control. The assessment is based on standard profile performance metrics and energy efficiency indicators obtained from MATLAB/Simulink simulations.

Table 5.3 Performance Comparison PID, Fuzzy and MPC controllers for Glaze firing

Criteria	PID Controller	Fuzzy logic Controller	MPC controller
IAE(^{o}c.s)	4.65 x 10^4	3.02 x 10^4	1.58 x 10^4
RMSE(^{o}c)	9.20	5.85	2.80
Max Error(^{o}c)	22.6	13.1	5.2
Overshoot %	2.75	0.98	0
Energy Index(kwh)	176.5	158.2	142.6
Power fluctuation	High	Medium	Low

Based on the results in Table 5.3, the Model Predictive Control (MPC) controller demonstrates the best overall performance for the glaze firing process, followed by the Fuzzy Logic Controller, while the PID controller performs the weakest. The PID controller exhibits the highest tracking errors, with IAE of 4.65×10^4 °C·s, RMSE of 9.20 °C, and a maximum error of 22.6 °C, indicating poor temperature profile tracking at high firing temperatures. Although overshoot is limited to 2.75%, the PID controller shows the highest energy consumption (176.5 kWh) and high power fluctuation, making it less suitable for energy-efficient and stable glaze firing.

The Fuzzy Logic Controller significantly improves tracking accuracy, reducing the IAE to 3.02×10^4 °C·s, RMSE to 5.85 °C, and maximum error to 13.1 °C, with a low overshoot of 0.98%. Energy consumption is also reduced to 158.2 kWh, accompanied by moderate power fluctuation. The MPC controller outperforms both alternatives, achieving the lowest IAE (1.58×10^4 °C·s), RMSE (2.80 °C), and maximum error (5.2 °C), with zero overshoot. Additionally, MPC records the lowest energy index (142.6 kWh) and smooth power behavior, making it the most accurate and energy-efficient control strategy for glaze firing.

CHAPTER SIX

CONCLUSION AND RECOMMENDATION

6.1 Conclusion

This thesis evaluated the performance of different temperature profile control strategies for an electric clay kiln used in the Ethiopian pottery industry. A mathematical model of the kiln was developed to capture its thermal behavior, including heat losses, time delay, and nonlinear effects. Using this model, PID, Fuzzy Logic Control (FLC), and Model Predictive Control (MPC) were designed and simulated in MATLAB/Simulink for bisque and glaze firing processes.

The results indicate that the conventional PID controller, despite its simplicity and wide industrial use, is not well suited for precise kiln temperature regulation. PID showed higher overshoot, IAE, RMSE, and greater energy consumption, especially during high-temperature glaze firing. These limitations arise from the kiln's large thermal inertia, nonlinear dynamics, and inherent time delay, which fixed-gain PID controllers cannot adequately manage.

Fuzzy Logic Control performed better than PID by providing smoother temperature tracking and reduced overshoot. Its ability to incorporate expert knowledge without relying on an exact mathematical model makes it robust and practical for small-scale and traditional pottery kilns where operating conditions may vary. Model Predictive Control demonstrated the best overall performance among the three controllers. MPC achieved superior tracking accuracy, minimal overshoot and improved energy efficiency for both firing stages. Its predictive capability and constraint-handling features allowed it to effectively manage the slow and complex thermal dynamics of the kiln. Although MPC requires higher computational resources and accurate modeling, its control performance makes it highly suitable for modern electric kilns.

Advanced control strategies particularly MPC and FLC offer significant improvements in temperature control, product quality, and energy efficiency. Their adoption can support the modernization and sustainability of the Ethiopian pottery industry while maintaining traditional production practices.

6.2 Recommendations

Based on the simulation results, it is recommended to adopt advanced temperature control techniques for clay kilns in the Ethiopian pottery industry. Model Predictive Control is highly suitable for electric kilns where high accuracy, energy efficiency, and product consistency are required. For small-scale and low-cost applications, Fuzzy Logic Control provides a practical and robust alternative to conventional PID controllers. Future studies should focus on:

- External disturbance such as ambient temperature variation, changes in clay load, door opening effects and power supply fluctuations this disturbance will improve temperature stability, firing accuracy and over all kiln performance.
- Practical implementation of the proposed controllers on a real electric clay kiln is strongly recommended to validate the simulation results and assess real time performance, robustness and energy consumption.
- In addition, the application of advanced control techniques such as neural networks, neuro fuzzy system, hybrid MPC-fuzzy controllers should be investigated and compare with PID, FLC, MPC to further enhance control accuracy and energy efficiency.

REFERENCES

[1] E. Of *et al.*, “School of Graduate Studies,” no. June, 2013.

[2] M. C. Schütt, “TECHNOLOGY , COMMUNICATION AND TRANSPORT Gas & Electric fired Kiln”.

[3] C. M. Sayers, “Journal of Geophysical Research : Solid Earth The Elastic Properties of Clay in Shales Journal of Geophysical Research : Solid Earth,” pp. 5965–5974, 2018, doi: 10.1029/2018JB015600.

[4] S. A. Hussnain *et al.*, “Thermal Analysis and Energy Efficiency Improvements in Tunnel Kiln for Sustainable Environment,” 2021.

[5] “THE ELECTRIC KILN (Harry Fraser)1994 (Z-Library).pdf.”

[6] G. Doktoringenieur *et al.*, “Solid-Solid Recuperation to Improve the Energy Efficiency of Tunnel Kilns,” 1979.

[7] E. Tsega, A. Mosisa, and F. Fufa, “Effects of Firing Time and Temperature on Physical Properties of Fired Clay Bricks,” vol. 5, no. 1, pp. 21–26, 2017, doi: 10.11648/j.ajce.20170501.14.

[8] S. L. City and S. L. City, “Factorial analysis of a c e m e n t kiln,” vol. 5, no. October, pp. 341–347, 1981.

[9] S. Aliyu, B. Garba, B. G. Danshehu, A. D. Isah, and S. Energy, “Studies On The Chemical And Physical Characteristics Of Selected Clay Samples,” vol. 2, no. 7, pp. 171–183, 2013.

[10] A. A. Kadir, A. Mohajerani, F. Roddick, and J. Buckeridge, “Density , Strength , Thermal Conductivity and Leachate Characteristics of Light-Weight Fired Clay Bricks Incorporating Cigarette Butts,” pp. 179–184, 2010.

[11] G. Stojanovski and M. Stankovski, *Advanced industrial control using fuzzy-model predictive control on a tunnel klin brick production*, vol. 44, no. 1 PART 1. IFAC, 2011. doi: 10.3182/20110828-6-IT-1002.00913.

[12] A. Eskelinen, A. Zakharov, S. L. Jämsä-Jounela, and J. Hearle, “Dynamic modeling of a multiple hearth furnace for kaolin calcination,” *AIChE J.*, vol. 61, no. 11, pp. 3683–3698, 2015, doi: 10.1002/aic.14903.

[13] Q. adar BakhshBaloch, “Temperature profile control of a multiple hearth furnace for khaolin calcinationTitle,” vol. 11, no. 1, pp. 92–105, 2017.

[14] J. Zhang, “Research on the Design of Ceramic Kiln Control System Based on PID,” vol. 59, pp. 709–714, 2017, doi: 10.3303/CET1759119.

[15] Y. Zhang, L. Li, Z. L. Wang, T. H. Xiao, and J. X. Huang, “Application and Research of Fuzzy PID Control in Resistance Furnace Temperature Control System,” *IOP Conf. Ser. Earth Environ. Sci.*, vol. 186, no. 5, 2018, doi: 10.1088/1755-1315/186/5/012051.

[16] G. Cantore, M. Milani, L. Montorsi, and F. Paltrinieri, “Modelling , Measurement and Control B Energy efficiency analysis of an entire ceramic kiln : A numerical approach,” vol. 87, no. 3, pp. 159–166, 2018.

[17] D. Machalek and K. M. Powell, “Model predictive control of a rotary kiln for fast electric demand response,” *Miner. Eng.*, vol. 144, 2019, doi: 10.1016/j.mineng.2019.106021.

[18] H. Baccour, M. Medhioub, F. Jamoussi, and T. Mhiri, “Influence of firing temperature on the ceramic properties of Triassic clays from Tunisia,” *J. Mater. Process. Technol.*, vol. 209, no. 6, pp. 2812–2817, 2009, doi: 10.1016/j.jmatprotec.2008.06.055.

[19] S. Weiner, A. Nagorsky, I. Taxel, Y. Asscher, and R. Maria, “Journal of Archaeological Science : Reports High temperature pyrotechnology : A macro- and microarchaeology study of a late Byzantine-beginning of Early Islamic period (7th century CE) pottery kiln from Tel Qatra / Gedera , Israel,” vol. 31, no. February, p. 102263, 2020.

[20] M. R. Ravi, P. L. Dhar, and S. Kohli, “Energy Audit and Improvement of an Updraught Pottery Kiln,” pp. 1–20.

[21] N. A. Tseligorov, A. V. Chubukin, A. K. Naser, D. V. Olkhovatov, and E. N. Tseligorova, “Modeling of the tunnel kiln control system taking into account the features of the pid controller and fuzzy logic,” *J. Phys. Conf. Ser.*, vol. 2131, no. 2, 2021, doi: 10.1088/1742-6596/2131/2/022022.

[22] K. Govind, P. U. Keerthidas, R. Karthik, and R. Kishore, “Design and Simulation of Pottery Kiln,” vol. 10, no. 2, pp. 1–16, 2022, doi: 10.4172/2321-6212.10.2.001.

[23] S. Raut *et al.*, “TRADITIONAL POTTERY KILNS FOR TERRACOTTA WARES,” pp. 1996–2003, 2022.

[24] O. R. Olabode, “Development of Fuzzy Logic Controller Based Temperature Control for Kiln Control,” vol. 6, no. 1, pp. 684–688, 2022.

[25] N. Shakya, B. Prajapati, and P. Raj, “Performance Analysis and Improvement of Existing Electric Resistance Furnace for Ceramic Sector in Thimi , Bhaktapur,” vol. 8914, pp. 725–732, 2022.

[26] T. Namaswa, D. F. R. P. Burslem, and J. Smith, “Bioresource Technology Reports Emerging trends in appropriate kiln designs for small-scale biochar production in low to middle income countries,” *Bioresour. Technol. Reports*, vol. 24, no. July, p. 101641, 2023, doi: 10.1016/j.biteb.2023.101641.

[27] C. Dechpratoom, A. Hokpunna, P. Yeunyongkul, and R. Munsin, “Numerical Simulation and Experimental Study of Thermal Distribution Behavior in Downdraft Ceramic Kiln,” no. 78, pp. 36–44, 2023.

[28] S. Cansee, A. Pattiya, and R. Resources, “Engineering and Applied Science Research during clay

brick firing," vol. 50, no. 5, pp. 405–412, 2023, doi: 10.14456/easr.2023.43.
[29] B. Laurini, N. Cantisani, W. R. L. da Silva, Y. Zong, and J. B. Jørgensen, "Electrification of Clay Calcination: A First Look into Dynamic Modeling and Energy Management for Integration with Sustainable Power Grids," no. 64021, 2024, [Online]. Available: http://arxiv.org/abs/2404.12695
[30] V. Cantavella, A. Moreno, A. Mezquita, and D. Llorens, "temperature Distribution inside a ceramic TILE during industrial firing," no. 1, pp. 147–160.
[31] D. Ferrer and T. Cerarnica, "STUDY OF TRANSVERSE TEMPERATURE GRADIENTS IN ROLLER KILNS UNDER DIFFERENT OPERATING CONDITIONS," pp. 295–308.
[32] V. Du Phan *et al.*, "Development of an Adaptive Fuzzy-Neural Controller for Temperature Control in a Brick Tunnel Kiln," *Electron.*, vol. 13, no. 2, 2024, doi: 10.3390/electronics13020342.
[33] S. Ferrari, I. Cuccui, P. Cerutti, O. Allegretti, and S. Ferrari, "A hybrid solar / biomass active indirect kiln dryer for timber in the Democratic Republic of Congo A hybrid solar / biomass active indirect kiln dryer for timber in the Democratic Republic of Congo," vol. 0750, 2024, doi: 10.1080/01430750.2024.2367109.
[34] L. Ceccarelli, C. Moletti, P. Gallo Stampino, M. Caruso, and G. Dotelli, "Ceramic experimental firing on clays for ceramic production in Umbria (Italy). Characterization of mineralogical transformations with temperature," *J. Archaeol. Sci. Reports*, vol. 65, no. September 2024, 2025, doi: 10.1016/j.jasrep.2025.105189.
[35] R. Fawzy, A. H. Mohammed, and E. Desouky, "Development of a Smart Ceramic Kiln Based on Effective Control of the Firing Process : An Applied Study," vol. 6, pp. 155–159, 2025, doi: 10.21608/SVUSRC.2025.376666.1279.
[36] C. Ionescu and D. Copot, "Hands-on MPC tuning for industrial applications," vol. 67, no. 5, pp. 925–945, 2019, doi: 10.24425/bpasts.2019.130877.
[37] V. K. Giri, "A Temperature Control Method of Electric Heating Furnace Based on Fuzzy PID A Temperature Control Method of Electric Heating Furnace Based on Fuzzy PID", doi: 10.1088/1742-6596/2503/1/012101.
[38] M. Kumavat and S. Thale, "Analysis of CSTR Temperature Control with PID , MPC & Hybrid MPC- PID Controller," vol. 01001, pp. 1–7, 2022.
[39] "COMPARISON BETWEEN MODEL PREDICTIVE CONTROL AND PID CONTROL," 2010.
[40] "Temperature Control of Electric Furnace for Glass Tempering Process Using Feed Forward Adaptive Control (Mrac)," 2020.
[41] X. Chen, "Temperature control in electric furnaces : Methods , applications , and challenges Temperature control in electric furnaces : Methods , applications , and challenges," 2023, doi:

10.1088/1742-6596/2649/1/012032.

[42] W. Paper, “Three Ways to Speed Up Model Predictive Controllers”.

[43] S. H. Zak, “Fall 2011 Model-based Predictive Control (MPC) Basic Structure of MPC,” pp. 1–26, 2011.

[44] P. Abinaya and P. Eee, “Performance Comparison of MPC and PID Controller for Single Input Single Output Process,” no. 1, 2019.

[45] F. M. Salem, “A comparative study of MPC and optimised PID control Mohamed I . Mosaad Mohamed A . Awadallah,” vol. 2, no. 4, pp. 242–250, 2015.

[46] A. M. Mahmood, “Design a Model Predictive Controller for an Electrical Furnace System,” vol. 32, no. 1, pp. 91–105, 2014.

[47] I. Applications, “Design and Implementation of Model Predictive Control Based PID Controller for Industrial Applications,” 2020.

[48] L. A. Bryan and E. A. Bryan, *PROGRAMMABLE CONTROLLERS THEORY AND IMPLEMENTATION*, Second Edi.

[49] A. N, “Fuzzy Sets and Decision Analysis,” no. 7, pp. 341–354, 2021.

[50] J. Sibigtroth, “Fuzzy Logic for Embedded Microcontrollers,” no. March, 1995.

Appendix

```
s = tf('s');

H = exp(-30*s)/(10800*s + 1);

G = pade(H, 1);   % 1st-order Padé

disp('After 1st-order Padé approximation:'); G
```